

Discovery of 2-[1-(4-Chlorophenyl)cyclopropyl]-3-hydroxy-8-(trifluoromethyl)quinoline-4-carboxylic Acid (PSI-421), a P-Selectin Inhibitor with Improved Pharmacokinetic Properties and Oral Efficacy in Models of Vascular Injury

Adrian Huang, Alessandro Moretto, Kristin Janz, Michael Lowe, Patricia W. Bedard, Steve Tam, Li Di, Valerie Clerin, Natalia Sushkova, Boris Tchernychev, Desiree H. H. Tsao, James C. Keith, Jr., Gray D. Shaw, Robert G. Schaub, Qin Wang, and Neelu Kaila*

Pfizer Global Research and Development, 200 Cambridge Park Drive, Cambridge, Massachusetts 02140

Received September 15, 2009

Previously, we reported the discovery of PSI-697 (**1a**), a C-2 benzyl substituted quinoline salicylic acid-based P-selectin inhibitor. It is active in a variety of animal models of cardiovascular disease. Compound **1a** has also been shown to be well tolerated and safe in healthy volunteers at doses of up to 1200 mg in a phase 1 single ascending dose study. However, its oral bioavailability was low. Our goal was to identify a back up compound with equal potency, increased solubility, and increased exposure. We expanded our structure–activity studies in this series by branching at the α position of the C-2 benzyl side chain and through modification of substituents on the carboxylic A-ring of the quinoline. This resulted in discovery of PSI-421 with marked improvement in aqueous solubility and pharmacokinetic properties. This compound has shown oral efficacy in animal models of arterial and venous injury and was selected as a preclinical development compound for potential treatment of such diseases as atherosclerosis and deep vein thrombosis.

Introduction

P-selectin is expressed on two cell types, activated endothelial cells and activated platelets, which play a significant and well documented role in vascular disease, making P-selectin the principal selectin to target in these indications.¹ Its ligand P-selectin glycoprotein ligand 1 (PSGL-1⁴) is expressed on the surface of most leukocytes. Binding of P-selectin to PSGL-1 promotes interaction of leukocytes with platelets and endothelial cells.^{2–5} As a result, elevated P-selectin expression on inflamed endothelial tissue results in increased accumulation of monocytes, neutrophils, and lymphocytes on the vessel wall. These cells secrete products that create a proinflammatory, hypercoagulable state and contribute to lesion growth and instability.⁶ In addition, increased accumulation of platelets occurs on the surface of the tethered leukocytes. Platelet accumulation can promote myointimal proliferation through the release of a variety of growth factors as well as provide a surface for the activation of coagulation cascades.⁷ Activated platelets can also directly adhere to the surface of damaged blood vessels and capture leukocytes in the blood to further promote occlusion.⁶ Several studies using knockout animal models or inhibitors have shown that inhibition of the P-selectin/PSGL-1 interaction results in reduction of atherosclerotic

lesion development, myointimal proliferation, venous thrombosis, and ischemia/reperfusion injury and enhanced fibrinolysis in a variety of organ systems.^{6,8} Thus, disruption of the P-selectin/PSGL-1 interaction has significant therapeutic potential in a variety of vascular settings. A number of selectin inhibitors have progressed to clinical trials. Bimosiamose⁹ and rPSGL-1-Ig/YSPSL¹⁰ are the most advanced selectin inhibitors in the clinic. The glycomimetic, Bimosiamose, is a pan-selectin inhibitor and rPSGL-1-Ig is a recombinant Ig-chimera form of P-selectin's natural ligand. In addition, several companies have ongoing discovery programs.^{11–14}

In general, poor bioavailability of carbohydrate-based drugs has been the major challenge in the development of an orally available selectin inhibitor, while biologics are limited to intravenous administration for acute interventions. We recently reported noncarbohydrate-based quinolines as P-selectin inhibitors via high-throughput screening.¹⁵ Subsequent optimization had led to identification of clinical candidate **1a** (PSI-697),¹⁶ a novel, orally available small molecule P-Selectin inhibitor. Unfortunately, in the phase 1 clinical trial, we did not achieve the desired pharmacokinetic profile (Figure 1). In light of human ex vivo data showing reduction in thrombus formation with **1a**, improving pharmacokinetic properties was considered a critical step in moving forward in clinical evaluation.¹⁶ In this paper, we wish to report our efforts on the development of the back-up compound, **1h** (PSI-421). Branching at the α position of the C-2 benzyl side chain improved pharmacokinetics, while modification of substituents on the carbocyclic A-ring of the quinoline conferred the desired improvement in aqueous solubility.

*To whom correspondence should be addressed. Phone: (617)665-5626. Fax: (617)665-5685. E-mail: neelu.kaila@pfizer.com.

^a Abbreviations: PSGL-1, P-selectin glycoprotein ligand-1; bimosiamose, 1,6-bis-[3-(3-carboxymethylphenyl)-4-(O-R-D-mannopyranosyl)-phenyl] hexane; sLex, sialyl Lewis x; SAR, structure–activity relationship; CYP, cytochrome P450; IVM, intravital microscopy; STD, saturation transfer difference.

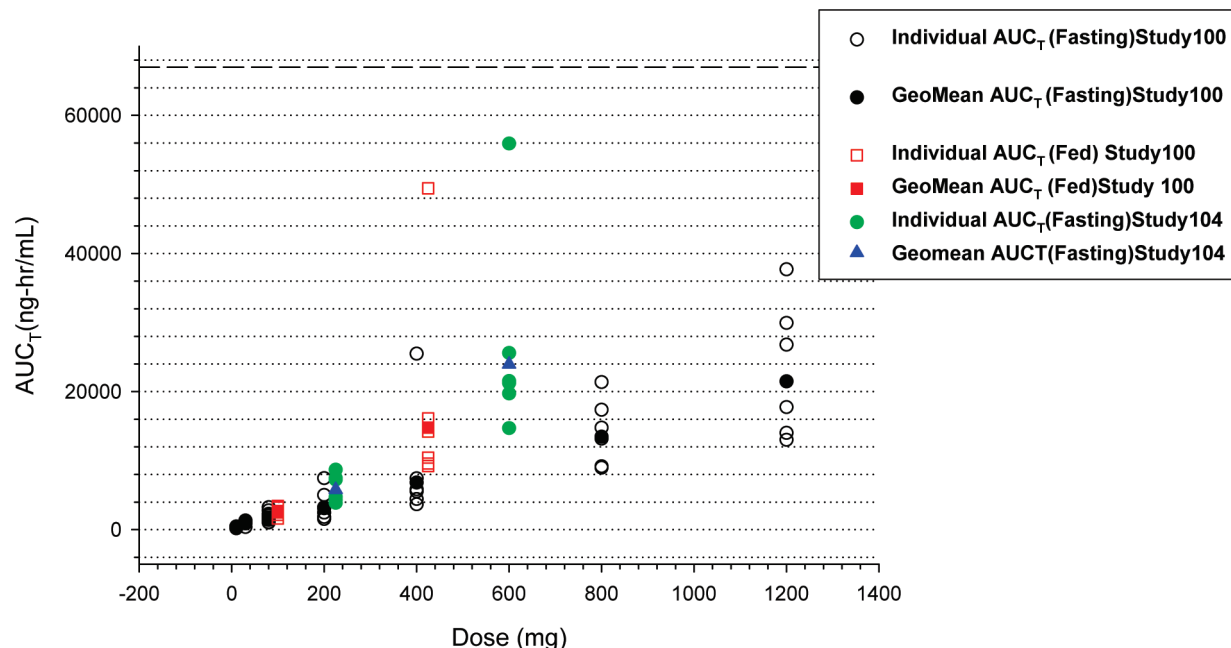
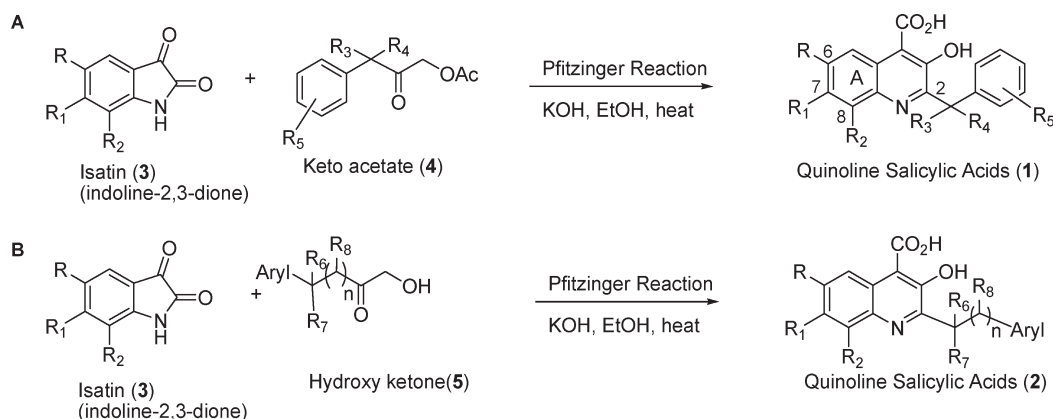


Figure 1. Individual and GeoMean AUC_T vs dose plots of **1a** (study administered under fasting and fed conditions).

Scheme 1



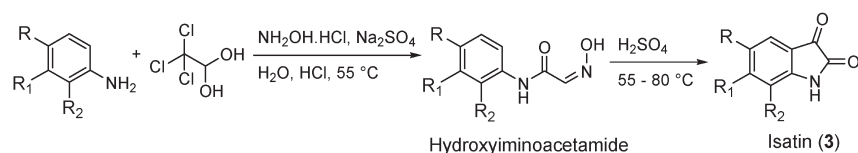
Chemistry

The target quinoline salicylic acids (**1**, **2**) were synthesized using the Pfitzinger reaction between an isatin (**3**, indoline-2,3-diones) and a keto acetate (**4**, Scheme 1A) or a hydroxy ketone (**5**, Scheme 1B), as described previously.^{15–17}

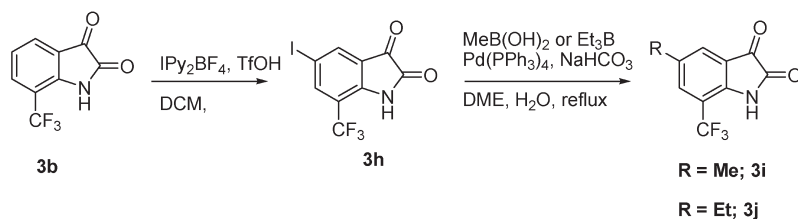
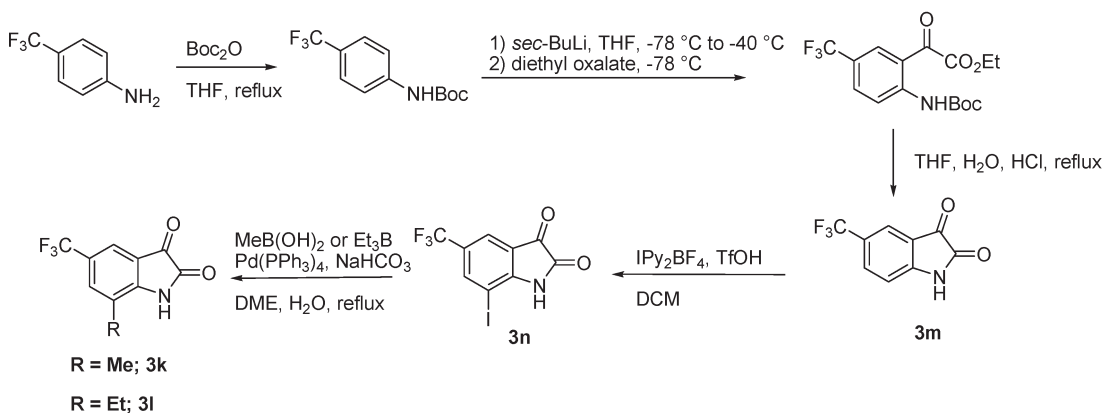
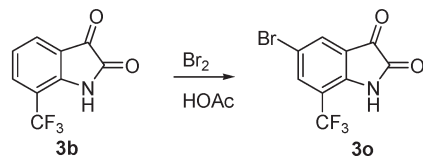
A few isatins were commercially available. Most were prepared either by the Sandmeyer method or a close variation of this method.¹⁸ Reaction of anilines with chloral hydrate and hydroxylamine hydrochloride (Scheme 2A), followed by cyclization of the resulting hydroxyiminoacetamide intermediates by heating in concentrated sulfuric acid, gave the isatin products. The 5-alkyl-7-(trifluoromethyl)isatins (**3i,j**) were prepared by Suzuki coupling of 5-iodo-7-(trifluoromethyl)isatin (**3h**) with methyl boronic acid or triethyl borane using conditions of Lisowski et al. (Scheme 2B).¹⁹ The yields were moderate, and 20–30% of the uncoupled deiodinated product was usually observed. The 5-iodo-7-(trifluoromethyl)isatin (**3h**) needed for the Suzuki coupling could not be prepared directly by the Sandmeyer method. It was prepared in two steps. First, 7-(trifluoromethyl)isatin (**3b**) was synthesized via the Sandmeyer route, then iodination was carried out using the Barluenga reagent, IPy_2BF_4 .²⁰ A similar scheme was

used to synthesize the 5-(trifluoromethyl)-7-alkylisatins (**3k,l**, Scheme 2C). The starting 5-(trifluoromethyl)isatin (**3m**) could not be prepared using the Sandmeyer reaction. However, we were able to prepare it via ortho-lithiation of the BOC-protected aniline and reaction of the aryllithium species with diethyl oxalate. Hydrolysis in aqueous acid removed the BOC protecting group and cyclization to the isatin occurred.²¹ The 5-bromo-7-(trifluoromethyl)isatin (**3o**) was synthesized by bromination of 7-(trifluoromethyl)isatin (**3b**) (Scheme 2D).

The keto acetates (**4**) for the Pfitzinger reaction were synthesized by Arndt–Eistert homologation of an acid chloride to give chloroketones, followed by acetate displacement (Scheme 3).¹⁶ The hydroxyl ketones (**5**) for the Pfitzinger reaction were prepared by Wissner reaction of the acid chloride with tris(trimethylsilyloxy)ethylene (Scheme 4).²² The Wissner–Pfitzinger route (Schemes 1B, 4) to quinoline salicylic acids is one step shorter than the commonly used Arndt–Eistert–Pfitzinger route (Schemes 1A, 3) and does not require the use of diazomethane, a particularly hazardous reagent. In cases where the Wissner–Pfitzinger methodology failed, specifically in cases where the aryl ring was ortho-substituted, the Arndt–Eistert–Pfitzinger methodology was used instead.

Scheme 2. (Sandmeyer)**A (Sandmeyer)**

	R	R ₁	R ₂
3a ¹⁶	H		
3b ¹⁶	H	H	CF ₃
3c	Cl	H	CF ₃
3d ¹⁵	H	CH ₃	CH ₃
3e ¹⁶	H	H	i-Pr
3f ¹⁶	H	H	Et
3g	H	H	C(CF ₃) ₂ OH

B**C****D**

The carboxylic acids (**6**) for the Arndt–Eistert and Wissner reactions were either commercially available or synthesized using Scheme 5. Commercially available aryl nitriles were treated with aqueous sodium hydroxide and 1-bromo-2-chloroethane under phase transfer conditions.²³ The resulting cyclopropylnitriles (**7**) were saponified to form the corresponding carboxylic acids **6**.

Results and Discussion

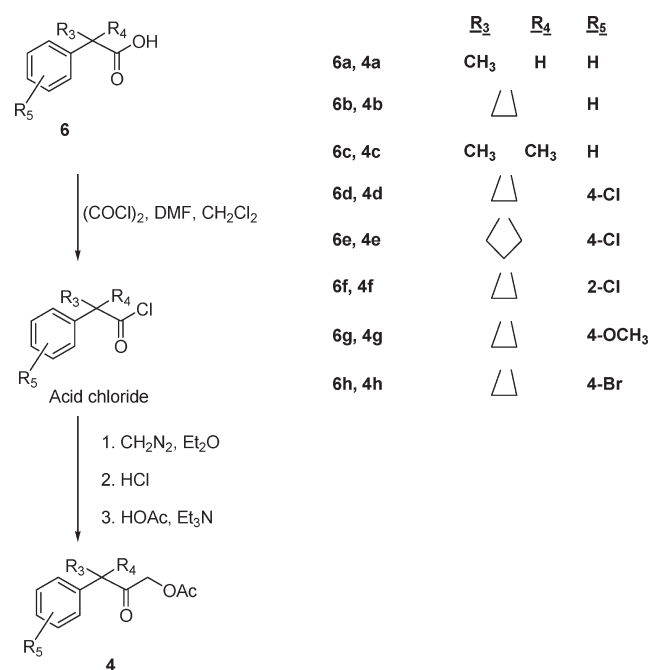
Compound **1a**, our first P-selectin development compound, was advanced into clinical studies in 2005. The compound was found to be well tolerated in phase I study, however, the oral exposure observed was below what was predicted by allometric species scaling from mouse, rat, and dog PK studies. Upon further analysis, the human data could be better

explained by inclusion of monkey PK in the allometric scaling. The goal of our back-up program was therefore to develop a candidate with good oral exposure in all four species. In addition, some improvement in human exposure of **1a** was achieved with formulation efforts; however, these efforts were limited by the poor aqueous solubility (Table 1). Therefore, one key consideration in our design was to greatly improve on the poor aqueous solubility of **1a**.

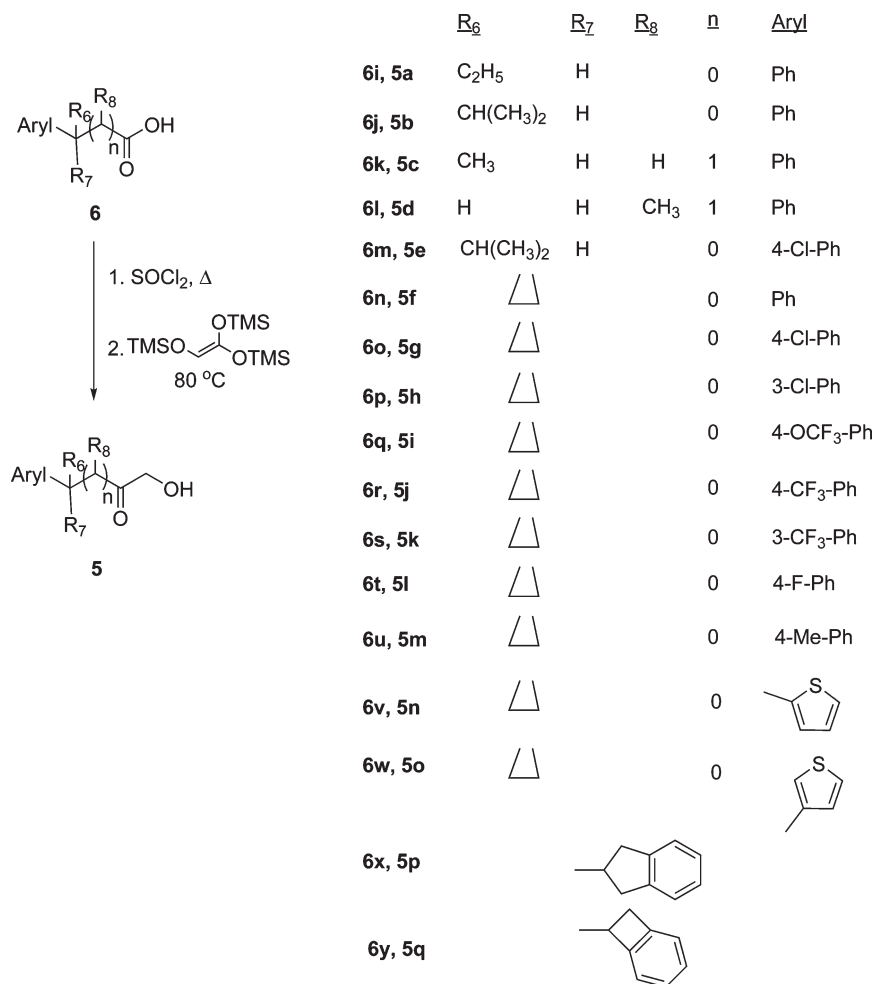
In our screening cascade, a Biacore assay is the primary potency filter. In this assay, soluble P-selectin near the K_d concentration for ligand binding is flowed over immobilized PSGL-1 with and without a small molecule inhibitor. The sensitivity of the Biacore instrument allows for measurement of the weak monomeric selectin interactions in real time under equilibrium flow conditions.^{24a} The natural ligand sialyl Lewis x (sLex) has an IC_{50} of approximately 15 mM in the

Biacore assay. It is well-demonstrated in the literature that selectin inhibitors show in vivo efficacy at approximately

Scheme 3. Arndt–Eistert Reaction



Scheme 4. Wissner Reaction



10-fold lower concentrations than their in vitro IC₅₀s. Examples of such correlations have been seen in the literature with biotherapeutic molecules such as rPSGL-Ig^{24a-c} and small molecules.^{15,24d} These molecules have in vitro and ex vivo IC₅₀s typically in the micromolar range but exhibit a markedly increased potency in vivo. TBC1269, which has an IC₅₀ of 70 μM in the P-selectin HL-60 cell assay^{24d} (sLex has an IC₅₀ of 3.4 mM in this assay), has shown activity in the kidney allograft rat model^{24e} and allergic sheep model^{24f} at a dose of 10 mg/kg IV and 10 mg aerosol, respectively. The major factors that may contribute to this paradox are in vivo flow rates and selectin densities, which are difficult to precisely reproduce using in vitro systems. In addition, the shear forces, cellular interactions, and variation in multimeric expression of receptor ligands seen with cell/cell interactions, both in vitro and in the more complicated in vivo systems, differ from the monomeric protein/protein interactions measured in the Biacore biochemical assay. The former may not require the same level of receptor occupancy for an effective outcome as required in the latter. These factors formed the basis for our rationale in pursuing micromolar selectin inhibitors.

Compounds that met the minimum potency criteria of >40% inhibition of P-selectin at 250 μM^{24g} in the Biacore assay and equilibrium solubility of 100 μg/mL at pH 6.6 (ref: **1a** 1 μg/mL) were taken forward for PK evaluation in rat. Compounds that show good oral exposure with AUC/dose >1500 ng·h/mL

were further evaluated for PK in other species and for efficacy in the in vivo models.

In our SAR study, we first evaluated the **1a** equity in the equilibrium solubility-pH profile assay. A plot of aqueous solubility (pH 6.6) versus P-selectin inhibition is shown in Figure 2. The 8-trifluoromethyl and -isopropyl substituted compounds had the optimum combination of aqueous solubility and P-selectin inhibition. Trifluoromethyl compounds did tend to exhibit slightly better solubility. Analogues with small alkyl groups (e.g., methyl, ethyl) at C-8 showed good solubility but loss in potency in the Biacore assay. The 7,8 fused ring, 7,8-dimethyl, C-8 large alkyl, and C-8 aryl substituted compounds all had good P-selectin inhibition but poor solubility, probably due to high lipophilicity.

Scheme 5

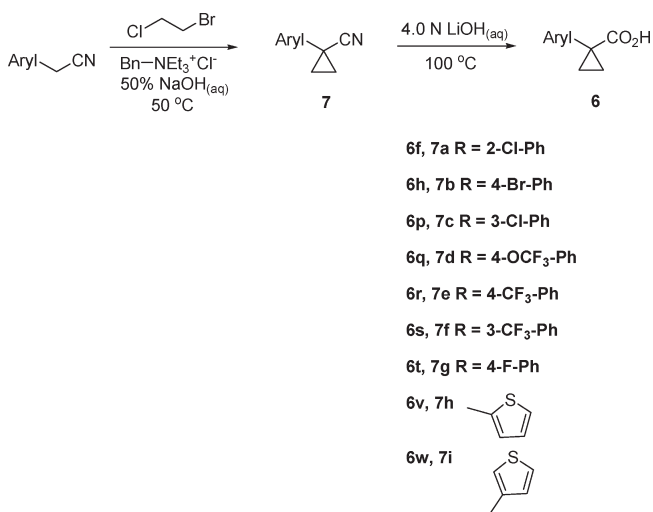


Table 1. Aqueous Solubility (mg/mL) of **1a** at Different pH

pH 1	pH 4.5	pH 6.6	pH 7.4	pH 9
< 0.001	< 0.001	< 0.001	0.09	0.075

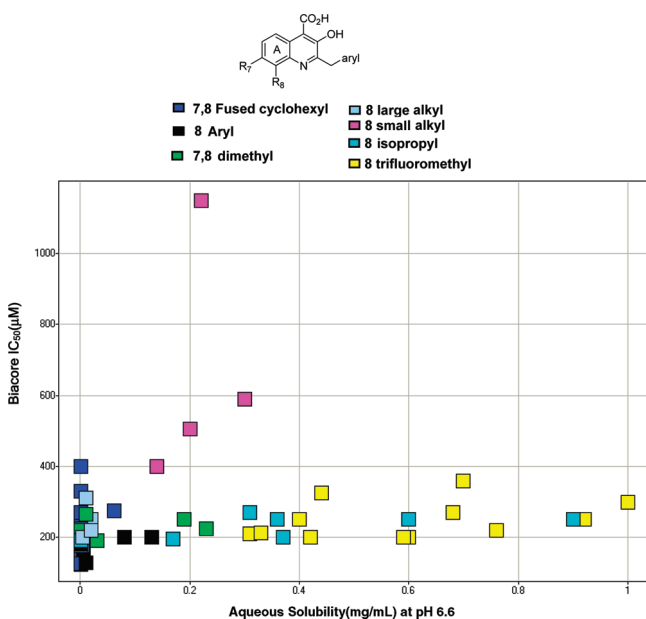


Figure 2. Effect of a ring substitution on aqueous solubility and P-selectin inhibition.

To improve the pharmacokinetic profile of the **1a** class of compounds, we next explored substitution at the potentially metabolically labile α position of the C-2 benzylic group (Table 2). The C-2-(1-phenylethyl) (**1c**) and C-2-(1-phenylcyclopropyl) (**1d**) analogues maintained potency and showed improved PO exposure and lower clearance in rats compared to **1a**.

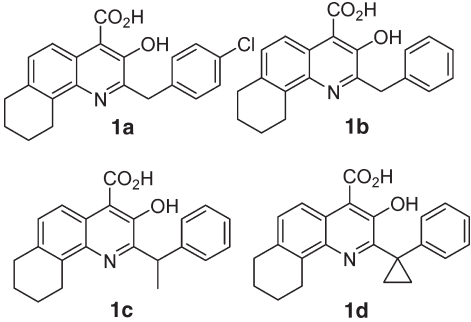
Next, we incorporated both solubility and PK enhancing features into the same molecules and built the 8-trifluoromethyl-2-(α -substituted benzyl) quinoline salicylic acid series. Results are shown in Table 3. Compounds with 1-phenylethyl (**1f**), 1-phenylpropyl (**2a**), 2-phenylpropyl (**1g**), and 1-aryl-cyclopropyl (**1h, 1i**) substitution at C-2 showed good potency and solubility. The 2-methyl-1-phenylpropyl analogues (**2b, 2e**) had good potency but poor solubility. Substitution with a medium-sized ring (**1j**) had a deleterious effect on potency. Extending the length of the linker between the quinoline and the C-2 phenyl ring (**2c** and **2d**) had little effect on potency. Replacement of the C-2 phenylcyclopropyl group with a thienylcyclopropyl (**2f, 2g**) was not tolerated. Compounds with bicyclic substituents at the C-2 position (**2h, 2i**) retained good potency and solubility. We selected the C-2 cyclopropyl moiety (**1h, 1i**) for exploring substitution on phenyl ring B (Table 4). Compounds with hydrophobic groups retained activity (**1h, 2j, 1j, 2l, 2m, 1m, 2n**), and increased polarity did not have a huge effect on potency (**2k, 1l**). The substituent's position on the phenyl ring had little effect on activity (**1h/2j/1k, 2l/2m**). All compounds showed acceptable aqueous solubility. A few additional series were synthesized by combining small alkyl groups at the eight position with different substituents (F, CF₃, Cl) on phenyl ring B.

As a further triage, lead compounds were tested in the CYP assays. In general, our series showed low inhibition (at 3 μ M) of 2D6 and 3A4 isoforms, but some potent inhibition was seen against CYP2C9 (> 50% at 3 μ M). To identify compounds that retained P-selectin inhibiting properties but were not inhibitors of CYP2C9, we studied substitution in the A ring. Because of their good aqueous solubility profile, small alkyl, alkoxy, and halogen groups were chosen for substitution at the 6-, 7- and 8-positions (Figure 3). A plot of CYP2C9 inhibition (% inhibition at 3 μ M) versus P-selectin inhibition (% inhibition at 250 μ M) for various A-ring analogues is shown in Figure 3. The 6-substituted analogues showed good CYP profiles but poor potency against P-Selectin. The C-8 analogues were potent inhibitors of P-selectin and CYP2C9. These two substitution patterns were combined and the disubstituted analogues evaluated in the Biacore and CYP2C9 assays (Table 5). Unfortunately, most compounds still showed moderate to high inhibition (> 45%) of CYP2C9. Compound **1n** was an exception but was not moved forward due to its poor aqueous solubility.

Twelve analogues with good potency and aqueous solubility were taken forward, and PK in Sprague–Dawley rats was evaluated (Table 6). In general, the compounds had low clearance, good exposure, and good bioavailability. Selected compounds with good exposure were evaluated in the acute intravital microscopy (IVM) mouse model.

In the IVM model, the exteriorization of the mouse cremaster muscle causes up-regulation of P-selectin, resulting in leukocyte rolling and adhesion on the inflamed vascular endothelium that can be visualized and quantitated via bright-field microscopy.^{16,17,25} Compounds were administered as a single oral dose of 50 mg/kg 35 min prior to measuring leukocyte rolling. Compounds **1h** and **1r** reduced leukocyte

Table 2. Alpha Substituted C-2 Benzyl Quinoline Salicylic acids as P-Selectin Inhibitors

				
	1a (PSI-697) ¹⁶	1b ¹⁶	1c	1d
Biacore IC ₅₀ (μM)	150	413	175	250
rat PK bioavailability (%)	27		66	45
clearance (mL/min/kg)	11		9	3.9
PO AUC/dose (h·ng/mL/mg)	440		1259	1925

rolling by 69 and 60%, respectively, relative to vehicle controls (Figure 5). Compound **1h** was selected for further evaluation.

Profiling of Compound **1h**

STD NMR. To confirm that our molecules bind directly to P-selectin, we conducted a saturation transfer difference (STD) NMR^{16,26} experiment using compound **1h** and P-LE (lectin domain of P-selectin). An STD of 9% was observed, confirming that **1h** binds to P-LE (Figure 4).

Physicochemical Properties. Solubility Profile (Table 7). Good solubility of **1h** was seen in buffer pH = 9.0 and simulated intestinal fluid (SIF). Moderate solubility of **1h** was seen in buffers of pH = 6.6 and 7.4 as well as in both (fed and fasted) simulated intestinal bile salts–lecithin mixture (SIBLM) fluids. **1h** was insoluble in buffers below pH 4.5.

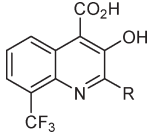
Solution Stability. Stability of **1h** was measured in physiological buffers (pH 1–9) and stimulated gastrointestinal (GI) fluids at 37 °C (Table 8). Within analytical variability, there was no change in drug concentration relative to the $t = 0$ value in all media evaluated for at least 24 h at 37 °C, indicating that the compound is stable over the duration of the experiment.

Permeability. The permeability of compound **1h** was measured across Caco-2 epithelial monolayers. Compound exhibited passive permeability. The apparent permeability (P_{app}) was medium [P_{app} (10^{-6} cm/s) A–B: 5.1; B–A: 9.8].

Predictive Toxicology. An in silico evaluation was conducted for **1h**. The current study utilized the Derek/Meteor program suite version 8.0 (Lhasa, Ltd.). **1h** and the majority of metabolites did not generate any alerts in Derek. In addition, non-GLP screening Ames test on **1h** was conducted. Results were negative.

Multispecies Microsomal Stability and Pharmacokinetics. In vitro metabolic studies with **1h** (Table 9) indicated high microsomal stability in all species tested. Compared to **1a**, compound **1h** showed improved microsomal stability in rat, monkey, and mouse, and this could be a result of eliminating/blocking metabolically labile sites in **1a**. The 7,8 fused cyclohexyl ring was replaced with a trifluoromethyl group, and the α position of the C-2 benzyl group was blocked as a cyclopropyl moiety in **1h**. Table 10 shows pharmacokinetics data for compound **1h** in male C57 mice, Sprague–Dawley rats, beagle dogs, and Cynomolgus monkeys. The results

Table 3. SAR at the Alpha Position of the C-2 Benzyl Quinoline Salicylic Acids

			
Compound	R	Biacore ^a %inh.@ 250 μM	Aq Solubility pH 6.6 (μg/mL)
1e ¹⁶	p-Cl-Ph	40	440
1f	Ph	50	1550
2a	Ph	55	600
2b	Ph	58	30
1g	Ph	44	2100
1h	p-Cl-Ph	55	920
1i	Ph	59	2810
2c	Ph	49	1550
2d	Ph	46	680
1j	p-Cl-Ph	0	
2e	p-Cl-Ph	≤10 ^b	Poor
2f	2-thiophene	15	
2g	3-thiophene	7	
2h	Indene	35	700
2i	Indene	45	800

^aThe interexperiment standard deviation of calculated percent inhibitions in the assay was ±5. The standard deviation between percent inhibitions calculated for two injections within the same assay was less than 1. ^bPoor inhibition due to low solubility in assay conditions.

indicate that the clearance was low in all four species, and exposure was high in rats, dogs, and monkeys and moderate in mice. When compared to **1a**, **1h** appeared to have an improved in vivo clearance, especially in rats and monkeys. The improved aqueous solubility of **1h** resulted in very good oral absorption in all species tested. The combination of reduced clearance and improved absorption yielded a high in vivo exposure. The in vitro metabolic data correlates well for rats, dogs, and monkeys. However, it does not show a good in vitro to in vivo correlation in mice. While we do not fully understand the cause for this discrepancy, one possibility could be due to the fact that a mouse iv study tends to have a larger intersubject variation (discrete dosing). When

compared to the clinical candidate **1a**, compound **1h** showed 50–70 fold increased oral exposure in rats and monkeys, which we hope will translate into better human exposure in the clinic.

IVM Rat. Since our balloon injury efficacy model is in rats, we decided to use the same species to study the dose response in the IVM model. Compound **1h** was administered by oral gavage at doses of 30, 15, 7.5, and 3 mg/kg 20 min prior to measuring leukocyte rolling; plasma samples were collected after rolling measurement. Doses of 30, 15, and 7.5 mg/kg gave a statistically significant decrease in the rolling flux of leukocytes in the cremasteric rat blood vessels compared with vehicle control (Figure 6). It is important to note that the inhibition of leukocyte rolling observed upon administration of compound **1h** at 7.5 mg/kg was comparable to that observed upon administration of a 4-fold higher dose (30 mg/kg) of **1a**.^{27,28}

Table 4. SAR of the Phenylcyclopropyl Quinoline Salicylic Acids

compd	R ₁	Biacore ^a		aq solubility pH 6.6 (μg/mL)
		%inh@250 μM		
1h	<i>p</i> -Cl	56		920
2j	<i>m</i> -Cl	66		300
1k	<i>o</i> -Cl	57		760
2k	<i>p</i> -OCF ₃	29		
1l	<i>p</i> -OCH ₃	26		
2l	<i>p</i> -CF ₃	47		200
2m	<i>m</i> -CF ₃	46		1000
1m	<i>p</i> -Br	64		420
2n	<i>p</i> -F	56		2900

^aThe interexperiment standard deviation of calculated percent inhibitions in the assay was ±5. The standard deviation between percent inhibitions calculated for two injections within the same assay was less than 1.

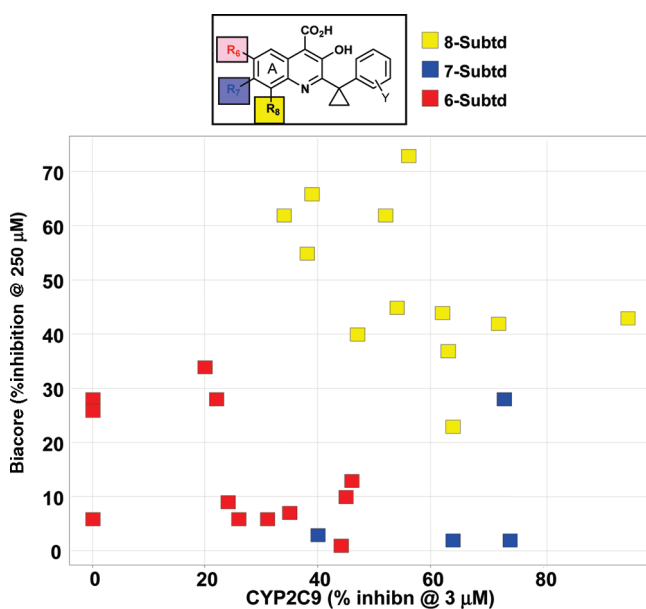


Figure 3. Effect of a ring substitution on inhibition of CYP2C9 and P-selectin.

The measured plasma concentration of **1h** following the 7.5 mg/kg dose was similar to that observed for **1a** after the 4-fold higher dose (Figure 7), which suggests that the superior efficacy of **1h** is due to its improved bioavailability. These results suggest that both compounds are effective at blocking the initial phase of leukocyte recruitment during an inflammatory process and confirm their ability to disrupt a P-selectin-dependent interaction.²⁹ It has been shown in the literature that the characteristic rolling of leukocytes relies on formation of multiple cooperative tethers.³⁰ It is hypothesized that this necessary cooperativity of tethers offers a rationale for in vivo efficacy of compounds with high protein binding and micromolar in vitro IC₅₀ values. Inhibition of a small fraction of the tethers is sufficient to prevent other tethers from holding under physiological flow.

Rat Carotid Artery Injury Model. To evaluate the effect on arterial injury with a more chronic dosing regimen, lead **1h** was tested in a rat carotid balloon injury model. This model is a widely used animal model of intimal hyperplasia or hyperproliferation of the smooth muscle cells lining the injured artery after angioplasty³¹ and is also representative of the myointimal process involved with formation of atherosclerotic lesions. P-Selectin dependence in this model has been demonstrated by using a neutralizing antibody to rat P-selectin, which reduced neointimal proliferation by 43%.³² Sprague–Dawley rats that underwent angioplasty of the left carotid artery were dosed with vehicle or **1h** at 30 mg/kg by oral gavage 1 h prior to arterial injury and once daily thereafter for 13 days. Histology of the carotid arteries showed that **1h** inhibited neointimal hyperplasia by 31% (Figure 8), which is approaching expected maximal inhibition observed in this model based on neutralizing antibody data.

Baboon DVT Model. In addition, we have previously shown³³ that oral administration of **1h** was efficacious in a baboon model of deep vein thrombosis (DVT) at a dose of 1 mg/kg. Primates treated with **1h** had greater percent vein opening and less vein wall inflammation than enoxaparin

Table 5. Disubstituted Quinoline Salicylic Acids

compd	R ₆	R ₇	R ₈	R	Biacore ^a	
					%inh@250 μM	CYP2C9% inh@3 μM
1n	Me	H	Me	H	20	54
2o	Me	H	CF ₃	H	40	87
2p	Et	H	CF ₃	H	40	86
2q	Me	H	Me	Me	11	55
2r	H	Me	Me	Me	24	47
2s	Me	H	Me	F	≤10 ^b	55
1o	Me	H	Me	Cl	47	17
2t	Me	H	CF ₃	Cl	65	72
2u	Et	H	CF ₃	Cl	≤10 ^b	81
1p	Cl	H	CF ₃	Cl	≤10 ^b	72
2v	Br	H	CF ₃	Cl	≤10 ^b	65
2w	CF ₃	H	Me	Cl	40	42
2x	CF ₃	H	Et	Cl	≤10 ^b	43

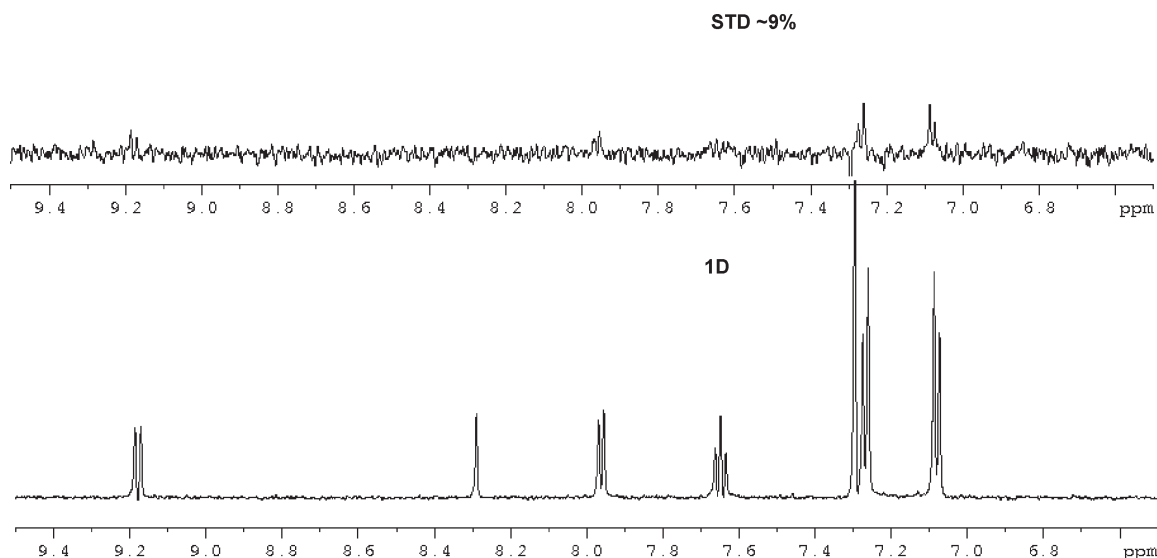
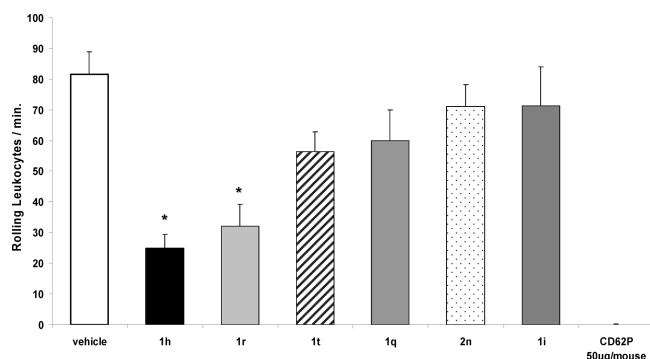
^aThe interexperiment standard deviation of calculated percent inhibitions in the assay was ±5. The standard deviation between percent inhibitions calculated for two injections within the same assay was less than 1. ^bPoor solubility under assay conditions.

Table 6. Pharmacokinetic Profile for Selected Phenylcyclopropyl Quinoline Salicylic Acids

compd	R ₁	R ₂	Biacore ^a		PK Rat ^b		PK Rat F%
			IC ₅₀ (μM)	Aq Solubility pH 6.6 (μg/mL)	PO AUC/Dose (ng.hr/mL/mg)	Clearance (mL/min/kg)	
1i			212	2810	1472	3.7	93
1h			225	920	21000	0.7	67
2h			357	700	340	28	49
1k			220	760	1336	2.4	19
2l			266	200	13800	0.4	31
2n			225	2900	14282	0.5	39
2y	8- <i>i</i> -Pr	<i>p</i> -F	187	2500	1263	8.7	65
2z	8-Et	<i>p</i> -CF ₃	205	250	2428	9.4	100
1q	8- <i>i</i> -Pr	H	198	370	2663	9	100
1r	8-C(CF ₃) ₂ OH	H	215	1500	5035	1	44
1s	7,8-dimethyl	<i>p</i> -Cl	236	190	1735	7	75
1t	8-Et	<i>p</i> -Cl	236	140	13986	2.4	100

^a The interexperiment standard deviation of calculated percent inhibitions in the assay was ±5. The standard deviation between percent inhibitions calculated for two injections within the same assay was less than 1. ^b Dose: iv 3 mpk; PO 10 mpk.

100μM Compound 1h; 5μM PLE

**Figure 4.** Compound **1h** binds to PLE, giving an STD of ~9%.**Figure 5.** Leukocyte rolling flux in cremasteric postcapillary venules in C57/BL6j mice after oral dosing with P-selectin inhibitors (50 mg/kg).

with no adverse effects on coagulation. Enoxaparin is a low molecular weight heparin (LMWH) which is the

Table 7. Solubility of **1h** in Physiological Buffers and Simulated GI Fluids

medium	solubility (mg/mL)
< pH 4.5 buffer	< LOD
pH 6.6 buffer	0.057
pH 7.4 buffer	0.165
pH 9.0 buffer	1.072
SIF	3.950
SIBLM (fed, pH 5.5)	0.835
SIBLM (fasted, pH 6.0)	0.087

standard of care for surgical DVT prophylaxis. It is a potent anticoagulant which can cause unwanted bleeding. The advantages of a P-selectin inhibitor are oral formulation, no adverse effects on coagulation, and equivalent or improved efficacy over LMWH. **1a** was also efficacious in this model, however at a higher dose, 30 mg/kg PO.^{34a} The improved bioavailability of **1h** allowed for a lower dose.

Compound **1h** has shown a clean profile in hERG and AMES testing. It has been advanced to predevelopment status.

Conclusion

We have successfully identified a back-up compound of the first generation P-selectin inhibitor **1a** with improved aqueous solubility and excellent pharmacokinetics properties in all four animal species: mouse, rat, dog, and monkey. With the improved oral bioavailability, **1h** has demonstrated good efficacy in three animal models: rat carotid balloon injury model, rat acute intravital microscopy (IVM) model, and baboon deep vein thrombosis model at a lower dose than **1a**. In addition a recent meta-analysis reported **1h** successfully paralleled the low-molecular-weight heparin enoxaparin for the treatment of DVT in nonhuman primate models by decreasing both thrombus burden and inflammation without causing bleeding complications or increasing coagulation times.^{34b} Compound **1h** is now in preclinical development.

Table 8. Physiological Stability^a of **1h** in Buffers (Percent Remaining)

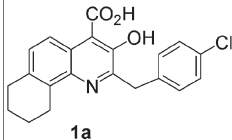
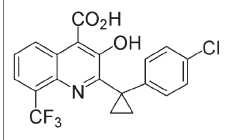
h	pH 1.0	pH 4.5	pH 6.6	pH 7.4	pH 9.0	SIF	SIBLM
0	100.0	100.0	100.0	100.0	100.0	100.0	100.0
4	101.1	101.5	101.8	101.6	98.5	101.4	101.7
8	101.5	101.6	104.3	102.4	98.0	103.7	100.7
12	101.7	99.2	105.7	102.3	98.8	101.1	101.2
16	101.7	100.7	103.1	102.0	98.7	100.6	101.8
20	101.5	100.3	102.5	102.3	101.1	99.4	103.1
24	100.8	101.5	103.6	102.7	99.6	95.0	102.8

^a Stability evaluated in presence of 20% acetonitrile.

Table 9. Microsomal Stability of Compound **1h** in Liver Microsomes

species	<i>T</i> _{1/2} (min)	
	1h	1a
S-D rats	> 60	2
beagle dogs	> 60	> 60
cyno monkeys	> 60	44
mouse	> 60	14
human	> 60	> 60

Table 10. Pharmacokinetic Properties of **1a**, **1h** in Mouse, Rat, Dog, and Monkey

*(ml/min/kg) **(hr*ng/ml/mg)	Mouse			Rat			Dog			Monkey		
	E		PO	E		PO	E		PO	E		PO
	F	Cl*	AUC/Dose**	F	Cl*	AUC/Dose**	F	Cl*	AUC/Dose**	F	Cl*	AUC/Dose**
 1a	100%	11.6	1510	27%	11	440	58%	0.9	11666	40%	5.6	1202
 1h	67% ^a	7	1505	88% ^b	0.7	21149	~100% ^a	0.9	28862	96% ^c	0.2	84620

^a Dose: iv 2 mpk, po 10 mpk. ^b Dose: iv 3mpk, po 25 mpk. ^c Dose: iv and po 5 mpk.

Experimental Section

Chemistry. Reactions were run using commercially available starting materials and solvents, without further purification. Proton NMR spectra were recorded at 300 MHz on a Varian Gemini 2000 or at 400 MHz on a Bruker AV-400 spectrometer using TMS (Figure 4). Combustion analyses were obtained using a Perkin-Elmer series II 2400 CHNS/O analyzer. CHN analyses were carried out by Robertson-Microlit. Where analyses are

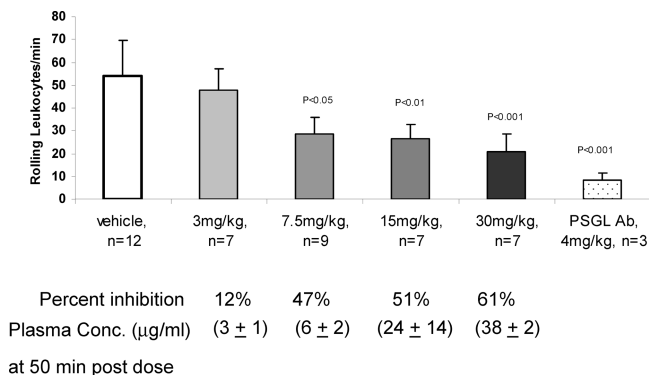


Figure 6. Leukocyte rolling flux in cremasteric postcapillary venules in rats after oral dosing with **1h**.

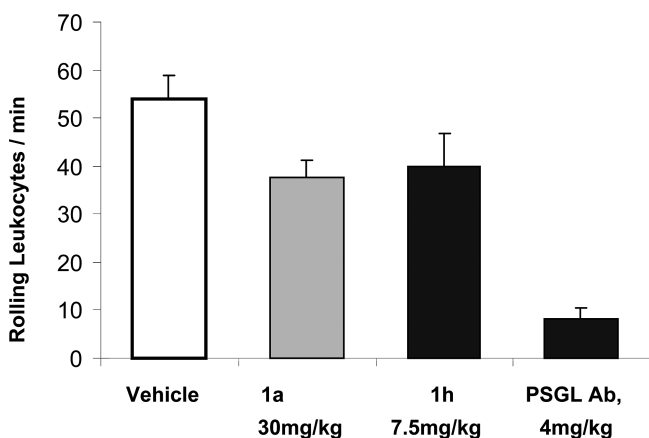


Figure 7. Leukocyte rolling flux in cremasteric post capillary venules in rat after oral dosing with **1a** and **1h**.

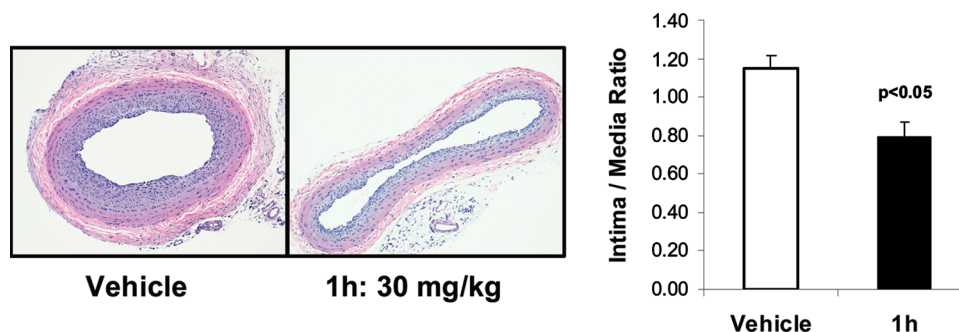


Figure 8. Efficacy of **1h** in rat carotid balloon injury model.

indicated by symbols of the elements, analytical results obtained for those elements were within 0.4 of the theoretical values. Low resolution mass spectra were obtained using a Micromass platform electrospray ionization quadrupole mass spectrometer. High resolution mass spectra were obtained using a Bruker APEXIII Fourier transform ion cyclotron resonance (FT-ICR) mass spectrometer equipped with an actively shielded 7 T superconducting magnet (Magnex Scientific, Ltd., UK) and an external Bruker APOLLO electrospray ionization (ESI) source. The microwave procedures were carried out with a Biotage microwave. Preparative HPLC was run using a Waters reverse phase prep HPLC with Xterra C18 5 mM, 30 mm \times 100 mm column. The flow rate was 40 mL/min and mobile phase A was water, mobile phase B was CH₃CN, and triethylamine was used as a modifier. Purity in H₂O–CH₃CN solvent systems was determined using an Agilent 1100 HPLC instrument, and all compounds analyzed were $\geq 95\%$ pure.

Synthesis of Keto Acetates (4a, 4b, 4c, 4d, 4e, 4f, 4g, 4h). The compounds were synthesized using the method described previously in detail.¹⁶ Synthesis details and characterization data listed in the Supporting Information.

1-Hydroxy-3-phenylpentan-2-one (5a). A mixture of carboxylic acid (2 g, 12.2 mmol) and 7 mL of thionylchloride in 15 mL of toluene was heated at 115 °C for 4–16 h (in some cases the reaction was done using thionyl chloride as a solvent and no toluene). Concentration of the reaction mixture gave an oily residue. To this residue was added 10 mL of toluene, and the resulting mixture was concentrated to yield a yellow oil. 1,1,2-Tris(trimethylsilyloxy)ethane (8.0 mL, 24.4 mmol) was added to the yellow oil. The reaction mixture was heated at 80–100 °C for 12–16 h under N₂. At 50 °C, 10 mL of dioxane and 2 mL of HCl (aq 1N) were added. The resulting mixture was stirred at 80 °C for 2 h. Concentration of the mixture gave a oily residue. Water (10 mL) and diethyl ether (15 mL) were added. The organic layer was washed with 5 mL of saturated NaHCO₃, brine, and dried over MgSO₄. The solid was removed via filtration. Concentration of the filtrate afforded the desired hydroxyl ketone as a yellow oil (80%). ¹H NMR (400 MHz, CDCl₃) δ 0.85 (t, J = 7.2 Hz, 3 H), 1.77–1.88 (m, 1 H), 2.09–2.17 (m, 1 H), 3.52 (t, J = 7.2 Hz, 1 H), 4.21 (d, J = 4.9 Hz, 2 H), 7.18–7.37 (m, 5 H).

Hydroxyl ketones (**5b–q**) were synthesized using the above procedure. Characterization data are listed in the Supporting Information.

1-(4-Bromophenyl)cyclopropanecarbonitrile (7b). To a 25 mL round-bottom flask equipped with a condenser was added 2-(4-bromophenyl)acetonitrile (0.794 g, 4.05 mmol, 1.0 equiv), 1-bromo-2-chloroethane (0.87 g, 6.08 mmol, 1.5 equiv), and triethylbenzyl ammonium chloride (0.018 g, 0.08 mmol, 0.02 equiv). The resulting mixture was heated to 50 °C in an oil bath, and sodium hydroxide (0.96 g, 24.0 mmol, 6.0 equiv) dissolved into 1.0 mL of water was added dropwise. The mixture was allowed to stir at 50 °C for 16 h. It was then allowed to cool to room temperature and poured into 50 mL of water. This suspension was extracted with three 25 mL portions of methylene chloride, and the combined organic layers then washed with

three 50 mL portions of 1.2 N HCl_(aq), three 50 mL portions of water, and 50 mL of saturated sodium chloride solution. The organic layer was then dried over magnesium sulfate, filtered, and the solvent removed in vacuo. The crude material was purified by Biotage Flash 40 to give the desired product cyclopropanecarbonitrile as a white solid (61%). ¹H NMR (400 MHz, cyclo CDCl₃) δ 1.33–1.44 (m, 2 H) 1.68–1.79 (m, 2 H) 7.16 (d, J = 8.59 Hz, 2 H) 7.48 (d, J = 8.84 Hz, 2 H).

Cyclopropanecarbonitriles (**7a**, **7c–i**) were synthesized using the above procedure. Characterization data listed in the Supporting Information.

1-(4-Bromophenyl)cyclopropanecarboxylic Acid (6h). To a 50 mL round-bottom flask equipped with a condenser was added 1-(4-bromophenyl)cyclopropanecarbonitrile (**7b**, 0.555 g, 2.5 mmol, 1.0 equiv) and 20 mL of 4.0 N LiOH_(aq). This suspension was heated to reflux in an oil bath and allowed to stir for 15 h. The resulting mixture was cooled to room temperature and poured into 250 mL of 1.2 N HCl. This suspension was extracted with three 75 mL portions of ethyl acetate, and the combined organic layer was washed with three 200 mL portions of water and 200 mL of saturated sodium chloride solution. The organic layer was then dried over magnesium sulfate, filtered, and the solvent removed in vacuo to give the desired cyclopropanecarboxylic acid as a white solid (95%). ¹H NMR (400 MHz, CDCl₃) δ 1.23 (q, J = 3.96 Hz, 2 H), 1.58–1.71 (m, 2 H), 7.21 (d, J = 8.34 Hz, 2 H), 7.43 (d, J = 8.34 Hz, 2 H).

Cyclopropanecarboxylic acids (**6f**, **6p–t**, **6v**, **6w**) were synthesized using the above procedure. Characterization data listed in the Supporting Information. Carboxylic acids **6a–e**, **6g**, **6i–o**, **6u**, **6x**, are commercially available.

Synthesis of Indolinediones (3c, 3g). The compounds were synthesized using method described previously in detail.¹⁶ Synthesis details and characterization data listed in the Supporting Information.

Iodo-7-(trifluoromethyl)indoline-2,3-dione (3h). Isatin **3b** (8.79 g, 40.9 mmol) was taken up in 105 mL of anhydrous dichloromethane in a 500 mL round-bottomed flask. Bis(pyridine)iodonium(I) tetrafluoroborate (23 g, 61 mmol) was added, followed by trifluoromethanesulfonic acid (10.8 mL, 18.4 g, 0.123 mol). The mixture was then stirred at room temperature for 40 min until LC-MS analysis showed complete disappearance of starting material. The solution was treated with 105 mL of water and extracted into dichloromethane (2 \times 45 mL). The combined organic extracts were washed with 5% aqueous sodium thiosulfate, dried over anhydrous magnesium sulfate, filtered, and evaporated to give pure product (12.0 g, 87% yield). ¹H NMR (400 MHz, DMSO-*d*₆) δ 8.03 (s, 1 H) 8.11 (s, 1 H) 11.55 (s, 1 H).

7-Iodo-5-(trifluoromethyl)indoline-2,3-dione (3n) was synthesized using the above procedure in 93% yield. ¹H NMR (400 MHz, DMSO-*d*₆) δ 7.80 (s, 1 H) 8.28 (dd, J = 1.8, 0.8 Hz, 1 H) 11.38 (s, 1 H).

5-Methyl-7-(trifluoromethyl)indoline-2,3-dione (3i). Isatin **3h** (1.12 g, 3.28 mmol) and tetrakis(triphenylphosphine)palladium (190 mg, 0.16 mmol) were taken up in 100 mL of ethylene glycol

dimethyl ether in a 500 mL round-bottomed flask. This solution was purged three times by opening to vacuum followed by back-filling with nitrogen. Next, methylboronic acid (390 mg, 6.6 mmol) was added, followed by a solution of sodium bicarbonate (0.55 g, 6.6 mmol) in 100 mL of water, and the evacuation/nitrogen backfill procedure repeated once more. The mixture was then heated to reflux, and analyzed by LC-MS analysis. After 1.5 h, no product had formed, so an additional 190 mg (0.16 mmol) of the palladium catalyst was added and the reaction allowed to reflux overnight. The organic solvent was then evaporated, and the remaining aqueous mixture partitioned between 100 mL each 2 M hydrochloric acid and ethyl acetate. The aqueous layer was extracted with additional ethyl acetate, and the combined organic extracts washed with brine, dried over anhydrous magnesium sulfate, filtered, and evaporated. The crude product was purified by flash chromatography over silica gel (0–6% ethyl acetate in dichloromethane) to give **3i** of sufficient purity to be used in the succeeding step (the product contained about 20% of the deiodinated side-product, 7-(trifluoromethyl)isatin). ¹H NMR (400 MHz, DMSO-*d*₆) δ 3.33 (s, 3 H) 7.62 (s, 1 H) 7.68 (s, 1 H) 11.35 (s, 1 H).

7-Methyl-5-(trifluoromethyl)indoline-2,3-dione (3k) was synthesized using the above procedure in 52% yield. ¹H NMR (400 MHz, DMSO-*d*₆) δ 2.27 (s, 3 H) 7.63 (s, 1 H) 7.82 (s, 1 H) 11.44 (s, 1 H).

5-Ethyl-7-(trifluoromethyl)indoline-2,3-dione (3j). The procedure described above for isatin **3i** was followed, reacting intermediate **3h** (1.47 g, 4.30 mmol) with a 1.0 M solution of triethylborane in tetrahydrofuran (8.6 mL, 8.6 mmol) in the presence of dichloro-[1,1'-bis(diphenylphosphino)ferrocene]palladium(II) dichloromethane adduct (176 mg, 0.215 mmol) and cesium carbonate (4.20 g, 12.9 mmol). Flash chromatography over silica gel (0–6% ethyl acetate in dichloromethane) gave product of sufficient purity to be used in the next step (0.417 g, 40% yield). ¹H NMR (400 MHz, DMSO-*d*₆) δ 1.17 (t, *J* = 7.6 Hz, 3 H) 2.65 (q, *J* = 7.6 Hz, 2 H) 7.66 (s, 1 H) 7.69 (s, 1 H) 11.35 (s, 1 H).

7-Ethyl-5-(trifluoromethyl)indoline-2,3-dione (3l) was synthesized using the above procedure in 38% yield. ¹H NMR (400 MHz, DMSO-*d*₆) δ 1.16 (t, *J* = 7.5 Hz, 3 H) 2.64 (q, *J* = 7.6 Hz, 2 H) 7.65 (s, 1 H) 7.80 (d, *J* = 0.8 Hz, 1 H) 11.45 (s, 1 H).

5-(Trifluoromethyl)indoline-2,3-dione (3m). This compound was synthesized using method described previously in detail.²¹ Synthesis details and characterization data listed in Supporting Information.

5-Bromo-7-(trifluoromethyl)indoline-2,3-dione (3o). Isatin **3b** (4.56 g, 21.2 mmol) was taken up in 45 mL of acetic acid in a 250 mL round-bottomed flask, and bromine (5.4 mL, 17 g, 0.11 mol) was added. The solution was stirred overnight at room temperature. LC-MS analysis showed that complete conversion to product had not occurred, so additional bromine was added (1.1 mL, 3.4 g, 21 mmol) and the reaction stirred an additional 5 h. It was then poured into an excess of ice and allowed to stand until the ice had melted. The precipitate was collected by filtration, washing repeatedly with water, and dried under vacuum to give fine, bright-orange crystals (5.12 g, 82% yield). ¹H NMR (400 MHz, DMSO-*d*₆) δ 7.96 (d, *J* = 2.0 Hz, 1 H) 8.04 (d, *J* = 2.0 Hz, 1 H) 11.59 (s, 1 H).

Quinoline salicylic acids (1, 2) were synthesized using method described previously in detail.²¹

3-Hydroxy-2-(1-phenylethyl)-7,8,9,10-tetrahydrobenzo[*h*]quinoline-4-carboxylic Acid (1c). Yellow powder (42%). ¹H NMR (400 MHz, DMSO-*d*₆) δ 1.68 (d, *J* = 6.8 Hz, 3 H) 1.75–1.96 (m, 4 H) 2.84 (t, *J* = 6.7 Hz, 2 H) 3.30 (t, *J* = 6.8 Hz, 1 H) 4.71–4.93 (m, 1 H) 7.14 (t, *J* = 8.0 Hz, 1 H) 7.20–7.29 (m, 3 H) 7.33 (d, *J* = 7.6 Hz, 2 H) 8.14–8.38 (m, 1 H). HRMS calcd for (C₂₂H₂₁NO₃ + H⁺) 348.1594, found 348.1593.

3-Hydroxy-2-(1-phenylcyclopropyl)-7,8,9,10-tetrahydrobenzo[*h*]quinoline-4-carboxylic Acid (1d). Yellow powder (14%). ¹H NMR (400 MHz, DMSO-*d*₆) δ 1.29–1.39 (m, 2 H) 1.44–1.56

(m, 2 H) 1.74–1.91 (m, 4 H) 2.84 (t, *J* = 5.43 Hz, 2 H) 3.26 (t, *J* = 6.06 Hz, 2 H) 7.10–7.17 (m, 3 H) 7.18–7.23 (m, 2 H) 7.28 (d, *J* = 8.59 Hz, 1 H) 8.36 (d, *J* = 9.35 Hz, 1 H). HRMS calcd for (C₂₃H₂₁NO₃ + H⁺) 360.1594, found 348.1595. Anal. (C₂₃H₂₁NO₃ · 0.5H₂O) C, H, N.

3-Hydroxy-2-(1-phenylethyl)-8-(trifluoromethyl)quinoline-4-carboxylic Acid (1f). Orange powder (36%). ¹H NMR (400 MHz, DMSO-*d*₆) δ 1.68 (d, *J* = 7.07 Hz, 3 H) 4.87 (q, *J* = 7.07 Hz, 1 H) 6.90–7.41 (m, 5 H) 7.69 (t, *J* = 6.82 Hz, 1 H) 7.97 (d, *J* = 6.82 Hz, 1 H) 8.84 (d, *J* = 8.34 Hz, 1 H). HRMS calcd for (C₁₉H₁₄F₃NO₃ + H⁺) 362.0999, found 362.0999. Anal. (C₁₉H₁₄F₃NO₃) C, H, N.

3-Hydroxy-2-(1-phenylpropyl)-8-(trifluoromethyl)quinoline-4-carboxylic Acid (2a). Light-yellow solid (28.7%). ¹H NMR (400 MHz, MeOH-*d*₄) δ 1.11 (t, *J* = 7.5 Hz, 3 H) 2.30–2.42 (m, 1 H) 2.64–2.77 (m, 1 H) 4.85 (t, *J* = 8.2 Hz, 1 H) 7.31–7.38 (m, 1 H) 7.40–7.48 (m, 2 H) 7.63 (d, 2 H) 7.85 (dd, *J* = 8.3, 7.6 Hz, 1 H) 8.14 (d, *J* = 7.6 Hz, 1 H) 9.29 (d, *J* = 8.3 Hz, 1 H). HRMS calcd for (C₂₀H₁₆F₃NO₃ + H⁺) 376.1155, found 376.1156.

3-Hydroxy-2-(2-methyl-1-phenylpropyl)-8-(trifluoromethyl)quinoline-4-carboxylic Acid (2b). White solid (16.0%). ¹H NMR (400 MHz, MeOH-*d*₄) δ 1.04 (d, *J* = 6.5 Hz, 3 H) 1.12 (d, *J* = 6.5 Hz, 3 H) 3.11–3.25 (m, 1 H) 4.57 (d, *J* = 10.6 Hz, 1 H) 7.28–7.34 (m, 1 H) 7.41 (dd, *J* = 7.2, 7.1 Hz, 2 H) 7.69 (d, *J* = 7.7 Hz, 1 H) 7.73 (d, *J* = 8.3 Hz, 2 H) 7.99 (d, *J* = 7.1 Hz, 1 H) 9.75 (d, *J* = 8.9 Hz, 1 H). HRMS calcd for (C₂₁H₁₈F₃NO₃ + H⁺) 390.1312, found 390.1311.

3-Hydroxy-2-(1-phenylcyclopropyl)-8-(trifluoromethyl)quinoline-4-carboxylic Acid (1g). Yellow solid (29%). ¹H NMR (400 MHz, MeOH-*d*₄) δ 1.68 (dd, *J* = 7.0, 4.7 Hz, 2 H) 7.46 (dd, *J* = 7.0, 4.7 Hz, 2 H) 7.51–7.59 (m, 2 H) 7.66 (dd, *J* = 8.6, 7.3 Hz, 2 H) 7.87 (dd, *J* = 8.4, 1.5 Hz, 1 H) 8.14 (d, *J* = 9.0 Hz, 1 H) 9.91 (d, *J* = 9.0 Hz, 1 H). HRMS calcd for (C₂₀H₁₄F₃NO₃ + H⁺) 374.0999, found 374.0987.

2-(1-(4-Chlorophenyl)cyclopropyl)-3-hydroxy-8-(trifluoromethyl)quinoline-4-carboxylic Acid (1h). Yellow solid (24.4%). ¹H NMR (400 MHz, MeOH-*d*₄) δ 1.58 (dd, *J* = 7.5, 4.6 Hz, 2 H) 1.82 (dd, *J* = 7.5, 4.6 Hz, 2 H) 7.44 (d, *J* = 8.7 Hz, 2 H) 7.53 (d, *J* = 8.7 Hz, 2 H) 7.87 (dd, *J* = 8.7, 7.6 Hz, 1 H) 8.14 (d, *J* = 7.6 Hz, 1 H) 9.29 (d, *J* = 8.7 Hz, 1 H). HRMS calcd for (C₂₀H₁₃ClF₃NO₃ + H⁺) 408.0609, found 408.061. Anal. (C₂₀H₁₃ClF₃NO₃) C, H, N.

3-Hydroxy-2-(2-phenylpropan-2-yl)-8-(trifluoromethyl)quinoline-4-carboxylic Acid (1i). Yellow powder (19%). ¹H NMR (400 MHz, DMSO-*d*₆) δ 1.78 (s, 6 H) 6.96–7.19 (m, 3 H) 7.19–7.30 (m, 2 H) 7.69 (t, *J* = 8.08 Hz, 1 H) 7.95 (d, *J* = 6.82 Hz, 1 H) 8.98 (d, *J* = 8.08 Hz, 1 H). HRMS calcd for (C₂₀H₁₆F₃NO₃ + H⁺) 376.1155, found 376.1154. Anal. (C₂₀H₁₆F₃NO₃) C, H, N.

3-Hydroxy-2-(1-phenylpropan-2-yl)-8-(trifluoromethyl)quinoline-4-carboxylic Acid (2c). Yellow solid (19.6%). ¹H NMR (400 MHz, MeOH-*d*₄) δ 1.50 (s, 3 H) 3.07 (dd, *J* = 13.4, 7.4 Hz, 1 H) 3.57 (dd, *J* = 13.4, 7.4 Hz, 1 H) 4.10–4.23 (m, 1 H) 7.25–7.42 (m, 5 H) 7.80 (dd, *J* = 8.5, 8.0 Hz, 1 H) 8.09 (d, *J* = 7.4 Hz, 1 H) 9.35 (d, *J* = 8.5 Hz, 1 H). HRMS calcd for (C₂₀H₁₆F₃NO₃ + H⁺) 376.1155, found 376.1139.

3-Hydroxy-2-(2-phenylpropyl)-8-(trifluoromethyl)quinoline-4-carboxylic Acid (2d). White solid (17.6%). ¹H NMR (400 MHz, MeOH-*d*₄) δ 1.56 (d, *J* = 7.1 Hz, 3 H) 3.47 (dd, *J* = 14.7, 8.4 Hz, 1 H) 3.64 (dd, *J* = 14.7, 6.7 Hz, 1 H) 3.85–3.96 (m, 1 H) 7.28–7.35 (m, 1 H) 7.43 (dd, *J* = 7.6, 7.6 Hz, 2 H) 7.50 (d, *J* = 7.6 Hz, 2 H) 7.82 (dd, *J* = 8.4, 7.6 Hz, 1 H) 8.10 (d, *J* = 7.6 Hz, 1 H) 9.26 (d, *J* = 8.4 Hz, 1 H). HRMS calcd for (C₂₀H₁₆F₃NO₃ + H⁺) 376.1155, found 376.1139. Anal. (C₂₀H₁₆F₃NO₃ · 0.1H₂O) C, H, N.

2-(1-(4-Chlorophenyl)cyclobutyl)-3-hydroxy-8-(trifluoromethyl)quinoline-4-carboxylic Acid (1j). White powder (50%). ¹H NMR (400 MHz, DMSO-*d*₆) δ 1.73–2.06 (m, 2 H) 2.55–2.78 (m, 2 H) 2.95–3.25 (m, 2 H) 7.35 (q, *J* = 8.34 Hz, 4 H) 7.69 (t, *J* = 7.96 Hz, 1 H) 7.97 (d, *J* = 7.58 Hz, 1 H) 8.92 (d, *J* = 8.59 Hz,

1 H). HRMS calcd for ($C_{21}H_{15}ClF_3NO_3 + H^+$) 422.0766, found 422.0759. Anal. ($C_{21}H_{15}ClF_3NO_3$) C, H, N.

2-[1-(4-Chloro-phenyl)-2-methyl-propyl]-3-hydroxy-8-trifluoromethyl-quinoline-4-carboxylic Acid (2e). Beige solid (10.8%). 1H NMR (400 MHz, DMSO- d_6) δ 0.80 (d, J = 6.57 Hz, 3 H), 0.86 (d, J = 6.82 Hz, 3 H), 2.76–2.89 (m, 1 H), 4.39 (d, J = 10.61 Hz, 1 H), 7.31 (d, J = 8.34 Hz, 2 H), 7.44 (d, J = 8.34 Hz, 2 H), 7.63 (dd, J = 8.34, 7.07 Hz, 1 H), 7.90 (d, J = 7.07 Hz, 1 H), 9.00 (d, J = 8.34 Hz, 1 H). HRMS calcd for ($C_{21}H_{17}ClF_3NO_3 + H^+$) 424.092, found 424.0924. Anal. ($C_{21}H_{17}ClF_3NO_3 \cdot 0.25H_2O$) C, H, N.

3-Hydroxy-2-(1-(thiophen-2-yl)cyclopropyl)-8-(trifluoromethyl)-quinoline-4-carboxylic Acid (2f). Yellow powder (31%). 1H NMR (400 MHz, DMSO- d_6) δ 1.33–1.43 (m, 2 H) 1.49–1.63 (m, 2 H) 6.82–6.85 (m, 1 H) 6.86–6.89 (m, 1 H) 7.24 (dd, J = 5.05, 1.26 Hz, 1 H) 7.61–7.74 (m, 1 H) 7.92 (d, J = 7.07 Hz, 1 H) 9.01 (d, J = 8.59 Hz, 1 H). HRMS calcd for ($C_{18}H_{12}F_3NO_3S + H^+$) 380.0563, found 380.0548. Anal. ($C_{18}H_{12}F_3NO_3S$) C, H, N.

3-Hydroxy-2-(1-(thiophen-3-yl)cyclopropyl)-8-(trifluoromethyl)-quinoline-4-carboxylic Acid (2g). Yellow powder (26%). 1H NMR (400 MHz, DMSO- d_6) δ 1.27–1.36 (m, 2 H) 1.39–1.55 (m, 2 H) 6.86 (dd, J = 4.93, 1.39 Hz, 1 H) 6.98 (dd, J = 2.91, 1.39 Hz, 1 H) 7.36 (dd, J = 5.05, 3.03 Hz, 1 H) 7.58–7.69 (m, 1 H) 7.87 (d, J = 7.07 Hz, 1 H) 9.15 (d, J = 8.59 Hz, 1 H). HRMS calcd for ($C_{18}H_{12}F_3NO_3S + H^+$) 380.0563, found 380.0548.

3-Hydroxy-2-indan-2-yl-8-trifluoromethyl-quinoline-4-carboxylic Acid (2h). Beige solid (16.1%). 1H NMR (400 MHz, DMSO- d_6) δ 3.34 (dd, J = 15.66, 8.59 Hz, 2 H) 3.43 (dd, J = 15.66, 8.08 Hz, 2 H), 4.26–4.38 (m, 1 H), 7.10–7.16 (m, 2 H), 7.22–7.28 (m, 2 H), 7.65 (dd, J = 8.94, 7.88 Hz, 1 H) 7.88 (d, J = 7.88 Hz, 1 H) 8.95 (d, J = 8.94 Hz, 1 H). HRMS calcd for ($C_{20}H_{14}F_3NO_3 + H^+$) 374.0999, found 374.1. Anal. ($C_{20}H_{14}F_3NO_3 \cdot 0.25H_2O$) C, H, N.

2-(1,2-Dihydrocyclobutabenzen-1-yl)-3-hydroxy-8-(trifluoromethyl)-quinoline-4-carboxylic Acid (2i). Yellow solid (5.8%). 1H NMR (400 MHz, MeOH- d_4) δ 3.46 (dd, J = 14.0, 5.6 Hz, 1 H), 3.98 (dd, J = 14.0, 3.1 Hz, 1 H), 5.06 (dd, J = 5.6, 3.1 Hz, 1 H), 6.99 (d, J = 6.3 Hz, 1 H), 7.04–7.09 (m, 2 H), 7.25 (d, J = 6.1 Hz, 1 H), 7.37–7.39 (m, 1 H), 7.62 (d, J = 7.3 Hz, 1 H), 9.50 (d, J = 8.6 Hz, 1 H). HRMS calcd for ($C_{19}H_{12}F_3NO_3 + H^+$) 360.0842, found 360.0847.

2-(1-(3-Chlorophenyl)cyclopropyl)-3-hydroxy-8-(trifluoromethyl)-quinoline-4-carboxylic Acid (2j). Yellow powder (15%). 1H NMR (400 MHz, DMSO- d_6) δ 1.32–1.42 (m, 2 H) 1.44–1.54 (m, 2 H) 6.95–7.37 (m, 4 H) 7.63 (t, J = 7.96 Hz, 1 H) 7.86 (d, J = 7.33 Hz, 1 H) 9.19 (d, J = 8.59 Hz, 1 H). HRMS calcd for ($C_{20}H_{13}ClF_3NO_3 + H^+$) 408.0609, found 408.0597. Anal. ($C_{20}H_{13}ClF_3NO_3 \cdot 0.5H_2O$) C, H, N.

2-(1-(2-Chlorophenyl)cyclopropyl)-3-hydroxy-8-(trifluoromethyl)-quinoline-4-carboxylic Acid (1k). Yellow powder (8%). 1H NMR (400 MHz, DMSO- d_6) δ 1.14–1.23 (m, 2 H) 1.77–1.89 (m, 2 H) 7.14–7.22 (m, 1 H) 7.23–7.33 (m, 2 H) 7.38–7.50 (m, 1 H) 7.61 (d, J = 7.07 Hz, 1 H) 7.72 (dd, J = 7.71, 1.64 Hz, 1 H) 9.61 (d, J = 8.08 Hz, 1 H). HRMS calcd for ($C_{20}H_{13}ClF_3NO_3 + H^+$) 408.0609, found 408.0598. Anal. ($C_{20}H_{13}ClF_3NO_3 \cdot 0.5H_2O$) C, H, N.

3-Hydroxy-2-(1-(4-(trifluoromethoxy)phenyl)cyclopropyl)-8-(trifluoromethyl)-quinoline-4-carboxylic Acid (2k). Yellow powder (33%). 1H NMR (400 MHz, DMSO- d_6) δ 1.33–1.44 (m, 2 H) 1.47–1.58 (m, 2 H) 7.19–7.25 (m, 2 H) 7.25–7.31 (m, 2 H) 7.60–7.76 (m, 1 H) 7.92 (d, J = 7.58 Hz, 1 H) 9.03 (d, J = 8.34 Hz, 1 H). HRMS calcd for ($C_{21}H_{13}F_6NO_4 + H^+$) 458.0822, found 458.0808. Anal. ($C_{21}H_{13}F_6NO_4 \cdot 0.5H_2O$) C, H, N.

3-Hydroxy-2-(1-(4-methoxyphenyl)cyclopropyl)-8-(trifluoromethyl)-quinoline-4-carboxylic Acid (1l). Yellow powder (17%). 1H NMR (400 MHz, DMSO- d_6) δ 1.18–1.32 (m, 2 H) 1.37–1.50 (m, 2 H) 3.68 (s, 3 H) 6.80 (d, J = 9.09 Hz, 2 H) 7.17 (d, J = 8.84 Hz, 2 H) 7.66 (dd, J = 8.59, 6.82 Hz, 2 H) 7.91 (d, J = 6.82 Hz, 1 H) 9.00 (d, J = 8.59 Hz, 1 H). HRMS calcd for ($C_{21}H_{16}F_3NO_4 + H^+$) 404.1104, found 404.1105.

3-Hydroxy-8-(trifluoromethyl)-2-(1-(4-(trifluoromethyl)phenyl)-cyclopropyl)quinoline-4-carboxylic Acid (2l). Yellow powder (33%). 1H NMR (400 MHz, $CDCl_3$) δ 1.39–1.51 (m, 2 H) 1.57–1.65 (m, 2 H) 7.34 (d, J = 8.08 Hz, 2 H) 7.60 (d, J = 8.34 Hz, 2 H) 7.65–7.78 (m, 1 H) 7.95 (d, J = 7.33 Hz, 1 H) 8.99 (d, J = 8.59 Hz, 1 H). HRMS calcd for ($C_{21}H_{13}F_6NO_3 + H^+$) 442.0873, found 442.0874. Anal. ($C_{21}H_{13}F_6NO_3$) C, H, N.

3-Hydroxy-8-(trifluoromethyl)-2-(1-(3-(trifluoromethyl)phenyl)-cyclopropyl)quinoline-4-carboxylic Acid (2m). Yellow powder (30%). 1H NMR (400 MHz, DMSO- d_6) δ 1.39–1.48 (m, 2 H) 1.52–1.62 (m, 2 H) 7.37–7.58 (m, 4 H) 7.67 (t, J = 8.34 Hz, 1 H) 7.92 (d, J = 7.07 Hz, 1 H) 9.05 (d, J = 8.34 Hz, 1 H). HRMS calcd for ($C_{21}H_{13}F_6NO_3 + H^+$) 442.0873, found 442.0866. Anal. ($C_{21}H_{13}F_6NO_3$) C, H, N.

2-(1-(4-Bromophenyl)cyclopropyl)-3-hydroxy-8-(trifluoromethyl)-quinoline-4-carboxylic Acid (1m). Yellow powder (24%). 1H NMR (400 MHz, DMSO- d_6) δ 1.28–1.38 (m, 2 H) 1.45–1.54 (m, 2 H) 7.12 (d, J = 8.59 Hz, 2 H) 7.41 (d, J = 8.59 Hz, 2 H) 7.63 (t, J = 8.59 Hz, 1 H) 7.86 (d, J = 7.33 Hz, 1 H) 9.18 (d, J = 8.59 Hz, 1 H). HRMS calcd for ($C_{20}H_{13}BrF_3NO_3 + H^+$) 452.0104, found 452.0106.

2-(1-(4-Fluorophenyl)cyclopropyl)-3-hydroxy-8-(trifluoromethyl)-quinoline-4-carboxylic Acid (2n). Yellow powder (14%). 1H NMR (400 MHz, DMSO- d_6) δ 1.24–1.35 (m, 2 H) 1.40–1.51 (m, 2 H) 6.93–7.12 (m, 2 H) 7.17–7.34 (m, 2 H) 7.62 (t, J = 8.08 Hz, 1 H) 7.86 (d, J = 7.33 Hz, 1 H) 9.17 (d, J = 9.60 Hz, 1 H). HRMS calcd for ($C_{20}H_{13}F_4NO_3 + H^+$) 392.0904, found 392.0908.

3-Hydroxy-6,8-dimethyl-2-(1-phenylcyclopropyl)quinoline-4-carboxylic Acid (1n). Yellow lyophilized powder (52%). 1H NMR (400 MHz, DMSO- d_6) δ 1.28–1.39 (m, 2 H) 1.45–1.59 (m, 2 H) 2.44 (s, 3 H) 2.69 (s, 3 H) 7.05–7.17 (m, 3 H) 7.17–7.25 (m, 2 H) 7.29 (s, 1 H) 8.17 (s, 1 H). HRMS calcd for ($C_{21}H_{19}NO_3 + H^+$) 334.1438, found 334.1437.

3-Hydroxy-6-methyl-2-(1-phenylcyclopropyl)-8-(trifluoromethyl)-quinoline-4-carboxylic Acid (2o). Yellow solid (10% yield). 1H NMR (400 MHz, DMSO- d_6) δ 1.33–1.39 (m, 2 H) 1.45–1.52 (m, 2 H) 2.55 (s, 3 H) 7.11–7.20 (m, 3 H) 7.21–7.27 (m, 2 H) 7.83 (d, J = 1.3 Hz, 1 H) 8.61 (s, 1 H). HRMS calcd for ($C_{21}H_{16}F_3NO_3 + H^+$) 388.1155, found 388.1155. Anal. ($C_{21}H_{16}F_3NO_3 \cdot 0.5H_2O$) C, H, N.

6-Ethyl-3-hydroxy-2-(1-phenylcyclopropyl)-8-(trifluoromethyl)-quinoline-4-carboxylic Acid (2p). Yellow solid (3.8% yield). 1H NMR (400 MHz, DMSO- d_6) δ 1.27 (t, J = 7.5 Hz, 3 H) 1.32–1.38 (m, 2 H) 1.46–1.51 (m, 2 H) 2.85 (q, J = 7.6 Hz, 2 H) 7.11–7.18 (m, 3 H) 7.20–7.26 (m, 2 H) 7.84 (d, J = 1.8 Hz, 1 H) 8.67 (s, 1 H). HRMS calcd for ($C_{22}H_{18}F_3NO_3 + H^+$) 402.1312, found 402.1314.

3-Hydroxy-6,8-dimethyl-2-(1-*p*-tolylcyclopropyl)quinoline-4-carboxylic Acid (2q). Yellow solid (55%). 1H NMR (400 MHz, DMSO- d_6) δ 1.29 (dd, J = 4.00, 2.00 Hz, 2 H) 1.46 (dd, J = 4.00, 2.00 Hz, 2 H) 2.22 (s, 3 H) 2.43 (s, 3 H) 2.69 (s, 3 H) 6.83–7.09 (m, 4 H) 7.27 (s, 1 H) 8.20 (s, 1 H). HRMS calcd for ($C_{22}H_{21}NO_3 + H^+$) 348.1594, found 348.1593. Anal. ($C_{22}H_{21}NO_3 \cdot 0.1H_2O$) C, H, N.

3-Hydroxy-7,8-dimethyl-2-(1-*p*-tolyl-cyclopropyl)-quinoline-4-carboxylic Acid (2r). Yellow solid (31.7%). 1H NMR (400 MHz, MeOD) δ 1.34 (dd, J = 7.2, 4.0 Hz, 2 H), 1.62 (dd, J = 7.2, 4.0 Hz, 2 H), 2.43 (s, 3 H) 2.47 (s, 3 H) 2.76 (s, 3 H) 7.15 (d, J = 8.5 Hz, 2 H) 7.20 (d, J = 8.5 Hz, 2 H) 7.30 (d, J = 9.0 Hz, 1 H) 8.97 (d, J = 9.0 Hz, 1 H). HRMS calcd for ($C_{22}H_{21}NO_3 + H^+$) 348.1594, found 348.1594.

2-(1-(4-Fluorophenyl)cyclopropyl)-3-hydroxy-6,8-dimethyl-quinoline-4-carboxylic Acid (2s). Yellow solid (52%). 1H NMR (400 MHz, DMSO- d_6) δ 1.32 (dd, J = 8.00, 4.00 Hz, 2 H) 1.49 (dd, J = 8.00, 4.00 Hz, 2 H) 2.43 (s, 3 H) 2.69 (s, 3 H) 7.04 (t, J = 8.59 Hz, 2 H) 7.20 (dd, J = 8.59, 5.56 Hz, 2 H) 7.28 (s, 1 H) 8.18 (s, 1 H). HRMS calcd for ($C_{21}H_{18}FNO_3 + H^+$) 352.1344, found 352.1345. Anal. ($C_{22}H_{18}FNO_3 \cdot 0.2H_2O$) C, H, N.

2-(1-(4-Chlorophenyl)cyclopropyl)-3-hydroxy-6,8-dimethylquinoline-4-carboxylic Acid (1o). Bright-yellow powder (27% yield). ^1H NMR (400 MHz, DMSO- d_6) δ 1.33–1.42 (m, 2 H) 1.47–1.57 (m, 2 H) 2.44 (s, 3 H) 2.69 (s, 3 H) 7.15 (dt, J = 9.0, 2.8 Hz, 2 H) 7.27 (dt, J = 9.1, 2.77 Hz, 2 H) 7.30 (s, 1 H) 8.13 (s, 1 H). HRMS calcd for ($\text{C}_{21}\text{H}_{18}\text{ClNO}_3 + \text{H}^+$) 368.1048, found 368.1049. Anal. ($\text{C}_{21}\text{H}_{18}\text{ClNO}_3 \cdot 0.1\text{H}_2\text{O}$) C, H, N.

2-(1-(4-Chlorophenyl)cyclopropyl)-3-hydroxy-6-methyl-8-(trifluoromethyl)quinoline-4-carboxylic Acid (2t). Pale-yellow solid. ^1H NMR (400 MHz, DMSO- d_6) δ 1.35–1.39 (m, 2 H) 1.50–1.54 (m, 2 H) 2.55 (s, 3 H) 7.18 (dt, J = 8.8, 2.5 Hz, 2 H) 7.29 (dt, J = 8.8, 2.5 Hz, 2 H) 7.83 (s, 1 H) 8.60 (s, 1 H). HRMS calcd for ($\text{C}_{21}\text{H}_{15}\text{ClF}_3\text{NO}_3 + \text{H}^+$) 422.0765, found 422.0758. Anal. ($\text{C}_{21}\text{H}_{15}\text{ClF}_3\text{NO}_3$) C, H, N.

2-(1-(4-Chlorophenyl)cyclopropyl)-6-ethyl-3-hydroxy-8-(trifluoromethyl)quinoline-4-carboxylic Acid (2u). Pale-yellow solid (14% yield). ^1H NMR (400 MHz, DMSO- d_6) δ 1.27 (t, J = 7.6 Hz, 3 H) 1.33–1.39 (m, 2 H) 1.48–1.54 (m, 2 H) 2.85 (q, J = 7.4 Hz, 2 H) 7.14–7.20 (m, 2 H) 7.25–7.32 (m, 2 H) 7.85 (d, J = 1.5 Hz, 1 H) 8.67 (s, 1 H). HRMS calcd for ($\text{C}_{22}\text{H}_{18}\text{F}_3\text{NO}_3 + \text{H}^+$) 402.1312, found 402.1314.

6-Chloro-2-(1-(4-chlorophenyl)cyclopropyl)-3-hydroxy-8-(trifluoromethyl)quinoline-4-carboxylic Acid (1p). Pale-yellow solid (2.5% yield). ^1H NMR (400 MHz, DMSO- d_6) δ 1.33–1.37 (m, 2 H) 1.48–1.52 (m, 2 H) 7.18 (ddd, 2 H) 7.28 (ddd, J = 8.8, 2.5, 2.3 Hz, 2 H) 7.90 (d, J = 2.3 Hz, 1 H) 9.20 (d, J = 2.0 Hz, 1 H). HRMS calcd for ($\text{C}_{20}\text{H}_{12}\text{Cl}_2\text{F}_3\text{NO}_3 + \text{H}^+$) 442.0219, found 442.0220.

6-Bromo-2-(1-(4-chlorophenyl)cyclopropyl)-3-hydroxy-8-(trifluoromethyl)quinoline-4-carboxylic Acid (2v). Yellow solid (3.5% yield). ^1H NMR (400 MHz, DMSO- d_6) δ 1.32–1.37 (m, 2 H) 1.48–1.52 (m, 2 H) 7.18 (ddd, J = 8.9, 2.5, 2.2 Hz, 2 H) 7.28 (ddd, J = 8.8, 2.4, 2.2 Hz, 2 H) 7.96 (d, J = 2.0 Hz, 1 H) 9.41 (d, J = 2.0 Hz, 1 H). HRMS calcd for ($\text{C}_{20}\text{H}_{12}\text{BrClF}_3\text{NO}_3 + \text{H}^+$) 485.9714, found 485.9729.

2-(1-(4-Chlorophenyl)cyclopropyl)-3-hydroxy-8-methyl-6-(trifluoromethyl)quinoline-4-carboxylic Acid (2w). Fuffy pale-yellow solid (6.6% yield). ^1H NMR (400 MHz, DMSO- d_6) δ 1.36–1.41 (m, 2 H) 1.55–1.59 (m, 2 H) 2.80 (s, 3 H) 7.15–7.20 (m, 2 H) 7.28 (ddd, J = 8.9, 2.5, 2.2 Hz, 2 H) 7.69 (s, 1 H) 8.99 (s, 1 H). HRMS calcd for ($\text{C}_{21}\text{H}_{15}\text{ClF}_3\text{NO}_3 + \text{H}^+$) 422.0765, found 422.0768. Anal. ($\text{C}_{21}\text{H}_{15}\text{ClF}_3\text{NO}_3 \cdot 0.4\text{H}_2\text{O}$) C, H, N.

2-(1-(4-Chlorophenyl)cyclopropyl)-8-ethyl-3-hydroxy-6-(trifluoromethyl)quinoline-4-carboxylic Acid (2x). Pale-yellow solid (16% yield). ^1H NMR (400 MHz, DMSO- d_6) δ 1.33 (t, J = 7.5 Hz, 3 H) 1.36–1.41 (m, 2 H) 1.52–1.57 (m, 2 H) 3.28 (q, J = 7.4 Hz, 2 H) 7.17–7.22 (m, 2 H) 7.26–7.31 (m, 2 H) 7.64 (d, J = 2.0 Hz, 1 H) 9.03 (s, 1 H). HRMS calcd for ($\text{C}_{22}\text{H}_{17}\text{ClF}_3\text{NO}_3 + \text{H}^+$) 436.0922, found 436.0921. Anal. ($\text{C}_{22}\text{H}_{17}\text{ClF}_3\text{NO}_3$) C, H, N.

2-(1-(4-Fluorophenyl)cyclopropyl)-3-hydroxy-8-isopropylquinoline-4-carboxylic Acid (2y). Yellow powder (39%). ^1H NMR (400 MHz, DMSO- d_6) δ 1.28–1.39 (m, 8 H) 1.43–1.53 (m, 2 H) 4.15–4.34 (m, 1 H) 6.94–7.12 (m, 2 H) 7.19–7.29 (m, 2 H) 7.41–7.47 (d, J = 8.08 Hz, 1 H) 7.48–7.56 (t, J = 8.08 Hz, 1 H) 8.40 (d, J = 8.08 Hz, 1 H). HRMS calcd for ($\text{C}_{22}\text{H}_{20}\text{FNO}_3 + \text{H}^+$) 366.15, found 366.1505.

8-Ethyl-3-hydroxy-2-(1-(4-(trifluoromethyl)phenyl)cyclopropyl)-quinoline-4-carboxylic Acid (2z). Yellow powder (13.4%). ^1H NMR (400 MHz, CDCl_3) δ 1.18–1.29 (m, 2 H) 1.36 (t, J = 7.20 Hz, 3 H) 1.40–1.47 (m, 2 H) 3.23–3.33 (m, 2 H) 7.40–7.46 (m, 3 H) 7.46–7.54 (m, 4 H) 8.58 (d, J = 8.45 Hz, 1 H). HRMS calcd for ($\text{C}_{22}\text{H}_{18}\text{F}_3\text{NO}_3 + \text{H}^+$) 402.1312, found 402.1310.

3-Hydroxy-8-isopropyl-2-(1-phenylcyclopropyl)quinoline-4-carboxylic Acid (1q). Yellow powder (40%). ^1H NMR (400 MHz, DMSO- d_6) δ 1.35 (d, J = 7.07 Hz, 6 H) 1.36–1.40 (m, 2 H) 1.43–1.53 (m, 2 H) 3.53–5.07 (h, J = 8.59 Hz, 1 H) 7.00–7.30 (m, 5 H) 7.40–7.48 (m, 1 H) 7.48–7.59 (m, 1 H) 8.37 (d, J = 8.59 Hz, 1 H). HRMS calcd for ($\text{C}_{22}\text{H}_{21}\text{NO}_3 + \text{H}^+$) 348.1594, found 348.1587. Anal. ($\text{C}_{22}\text{H}_{21}\text{NO}_3 \cdot 0.1\text{H}_2\text{O}$) C, H, N.

8-(1,1,1,3,3,3-Hexafluoro-2-hydroxypropan-2-yl)-3-hydroxy-2-(1-phenylcyclopropyl)quinoline-4-carboxylic Acid (1r). Yellow powder (30%). ^1H NMR (400 MHz, DMSO- d_6) δ 1.33–1.40 (m, 2 H) 1.40–1.49 (m, 2 H) 7.13–7.30 (m, 5 H) 7.65–7.71 (m, 1 H) 7.72–7.79 (m, 1 H) 9.06 (d, J = 8.34 Hz, 1 H). HRMS calcd for ($\text{C}_{22}\text{H}_{17}\text{F}_6\text{NO}_5 + \text{H}^+$) 472.0978, found 472.0956. Anal. ($\text{C}_{22}\text{H}_{17}\text{F}_6\text{NO}_5 \cdot \text{H}_2\text{O}$) C, H, N.

2-(1-(4-Chlorophenyl)cyclopropyl)-3-hydroxy-7,8-dimethylquinoline-4-carboxylic Acid (1s). Yellow solid (29.7%). ^1H NMR (400 MHz, CDCl_3) δ 1.34 (dd, J = 7.2, 4.0 Hz, 2 H), 1.62 (dd, J = 7.2, 4.0 Hz, 2 H), 2.43–2.47 (s, 3 H), 2.74–2.78 (s, 3 H), 7.15 (d, J = 8.5 Hz, 2 H), 7.20 (d, J = 8.5 Hz, 2 H), 7.30 (d, J = 9.0 Hz, 1 H), 8.97 (d, J = 9.0 Hz, 1 H). HRMS calcd for ($\text{C}_{21}\text{H}_{18}\text{ClNO}_3 + \text{H}^+$) 368.1048, found 368.1049.

2-(1-(4-Chlorophenyl)cyclopropyl)-8-ethyl-3-hydroxyquinoline-4-carboxylic Acid (1t). Acidification of the purified product did not give a solid precipitate, so the aqueous acetonitrile mixture was extracted into ethyl acetate and the extract evaporated and lyophilized to give a fluffy, bright-yellow solid (18% yield). ^1H NMR (400 MHz, DMSO- d_6) δ 1.32 (t, J = 7.5 Hz, 3 H) 1.36–1.42 (m, 2 H) 1.50–1.61 (m, 2 H) 3.23 (q, J = 7.5 Hz, 2 H) 7.19 (d, 2 H) 7.29 (d, J = 8.6 Hz, 2 H) 7.45 (d, 1 H) 7.51 (t, 1 H) 8.35 (d, J = 8.3 Hz, 1 H). HRMS calcd for ($\text{C}_{21}\text{H}_{18}\text{ClNO}_3 + \text{H}^+$) 368.1048, found 368.1048. Anal. ($\text{C}_{21}\text{H}_{18}\text{ClNO}_3$) C, H, N.

Biacore P-Selectin/PSGL-1 Inhibition Assay. Surface plasmon resonance (Biacore) assays were performed on a Biacore 3000 instrument (Biacore Inc., Piscataway, NJ) as described in ref 28. Briefly, a biotinylated, truncated form of PSGL-1 was immobilized on a Biacore SA sensor chip (Biacore Inc.). A truncated recombinant construct of P-selectin (P.LE) was flowed over the chip in the presence and absence of small molecule inhibitor. Final concentrations of reagents were 500 nM P-LE, 31.25–250 μM inhibitor, 10% dimethyl sulfoxide, and 1 \times Biacore buffer (100 mM HEPES, 150 mM NaCl, 1 mM CaCl_2 , 1 mM MgCl_2 , pH 7.4).

Solubility Assay. The compounds were equilibrated with pH buffers (0.1 M, ionic strength 0.15 M) at room temperature for 24 h. The solutions were filtered or centrifuged to remove the particulates. The filtrates or supernatants were diluted and assayed using LC-MS. The solubility is calculated against a standard curve.

Microsomal Stability Assay. The compounds were assayed using method described previously in detail.³⁵

CYP450 Inhibition Assay. The compounds were assayed using fluorescent method described previously in detail.³⁶ Percent inhibition was determined at 3 μM .

Caco-2 Permeability Assay. The compounds were assayed using method described previously in detail.³⁷

NMR Experiments. The NMR samples were prepared in D_2O buffer with 20 mM imidazole, pH 7.4, 150 mM NaCl, 5 mM CaCl_2 , and 0.02% NaN_3 . All experiments were performed at 25 $^\circ\text{C}$ in a Bruker Avance equipped with cryoprobe. The STD experiments were performed with a 100 μM nominal concentration of compound and 3 μM of the dimeric form of P-selectin (P-selectin Ig chimera). All experiments were performed at 25 $^\circ\text{C}$ in a Bruker Avance equipped with cryoprobe. For the STD experiment, on-resonance saturation was at 0.5 ppm and off-resonance was at -10 ppm. The saturation was performed with a 50 ms Gaussian-shaped pulse for 2 s. Data were processed with Bruker software Xwinnmr. Control STD experiments were performed with only the compound present in the sample.

Pharmacokinetic Studies. The animals used in the pharmacokinetic (PK) studies were male Cynomolgus monkeys, C57 mice, Sprague–Dawley rats, and beagle dogs. The PK studies were performed at Wyeth Research Laboratory (Andover, MA and Chazy, NY) under the supervision of the Institutional Animal Care and Use Committee. The formulation for iv administration was 20% DMSO/80% poly(ethylene glycol) 400 (PEG 400, v/v) for mice (5 mL/kg) and monkeys (1 mL/kg), 50% DMSO/50% PEG 400 (v/v, 1 mL/kg) for rats, and 100% DMSO

(0.05 mL/kg) for dogs, respectively. The oral formulation was an aqueous suspension containing 2% polysorbate 80 and 0.5% methylcellulose for all studies. Blood samples were collected over 24 h after iv or oral administration. Plasma samples were harvested and stored at -80°C until analysis. Plasma samples (50 μL) was precipitated with 100 mL of acetonitrile containing 500 ng/mL of internal standard, which had a similar chemical structure as that for the test article. The samples were vortexed and centrifuged at 5700 rpm for 10 min. Supernatants were subjected to LC-MS/MS analysis. HPLC separation was performed on a Perkin-Elmer series 200 HPLC system (Perkin-Elmer, Norwalk, CT) using an XTerra MS C18 column (2.1 mm \times 20 mm, 2.5 μm ; Waters, Milford, MA). The detection of test articles was performed on a PESCIEX API-3000 triple quadrupole mass spectrometer (Applied Biosystems, Concord, Ontario, L4K4 V8) using a TurboIon Spray source. The pharmacokinetic parameters were determined using WinNonlin (version 4.1, Pharsight, Mountain View, CA). Calculations were performed using the noncompartmental analysis approach (model 200 for the oral data and model 201 for the IV data).

Intravital Microscopy, Rat. Male Sprague–Dawley rats were divided into four treatment groups: vehicle, drug, and as a positive control, anti-rat-PSGL-1 antibody 4 mg/kg. Twenty minutes after dose administration, the cremaster muscle was surgically exteriorized and observed through an intravital microscope as described in (ref 28). The average number of rolling leukocytes was determined over 1 min in 10 vessels. Immediately after measurements (1 h postdosing), blood was collected from the inferior vena cava into tubes containing EDTA from each drug treated animal for determination of drug concentration. Mouse: The above procedure was repeated using C57B6 mice and 50 μg /mouse of P-selectin antibody was used as a positive control.

Rat Carotid Balloon Injury Model. Male Sprague–Dawley rats underwent angioplasty of the left carotid artery by the intraluminal passage of a balloon catheter as described in ref 28. Rats were treated orally with vehicle or 1h at 30 mg/kg formulated in methylcellulose/Tween 1 h before surgery and once/day for 13 days following surgery. Histology was performed in the carotid arteries 14 days after injury. Transverse tissue sections were stained with hematoxylin and eosin, and the intimal and the medial areas were then quantified morphometrically. Results were expressed as the average ratio of the intimal areas to the medial areas.

Statistical Analysis. In vivo pharmacology results are expressed as mean \pm standard error of the mean (SEM). Parameters of interest were subjected to analysis of variance (ANOVA) with a Tukey post hoc testing. GraphPad Prism software was used for analyses. Differences were considered significant if $P < 0.05$.

Acknowledgment. We thank Jerauld Skotnicki, John Potoski, and Alex Gontcharov from the DSC for their synthetic expertise, Uday Jain from PCC for physiological stability studies, DAC for spectral data and Yuanhong Li from the Structural Biology group for her assistance with protein NMR. We also thank Xu Meng, Arie Katz, Kathy Weisel, and Brinda Tammara for the 1a SAD data.

Supporting Information Available: Experimental procedures and analytical data for intermediates. This material is available free of charge via the Internet at <http://pubs.acs.org>.

References

- (1) (a) Andre, P. P-Selectin in haemostasis. *Br. J. Haematol.* **2004**, *126*, 298–306. (b) Blann, A. D.; Nadar, S. K.; Lip, G. Y. H. The adhesion molecule P-selectin and cardiovascular disease. *Eur. Heart J.* **2003**, *24*, 2166–2179.
- (2) Moore, K. L. Structure and function of P-selectin glycoprotein ligand-1. *Leukemia Lymphoma* **1998**, *29*, 1–15.
- (3) Vandendries, E. R.; Furie, B. C.; Furie, B. Role of P-selectin and PSGL-1 in coagulation and thrombosis. *Thromb. Haemostasis* **2004**, *92*, 459–466.
- (4) Yang, J.; Furie, B. C.; Furie, B. The biology of P-selectin glycoprotein ligand-1: its role as a selectin counterreceptor in leukocyte-endothelial and leukocyte-platelet interaction. *Thromb. Haemostasis* **1999**, *81*, 1–7.
- (5) McEver, R. P.; Cummings, R. D. Perspectives series: cell adhesion in vascular biology. Role of PSGL-1 binding to selectins in leukocyte recruitment. *J. Clin. Invest.* **1997**, *100*, 485–491.
- (6) Blann, A. D.; Nadar, S. K.; Lip, G. Y. The adhesion molecule P-selectin and cardiovascular disease. *Eur. Heart J.* **2003**, *24*, 2166–2179.
- (7) Steinhubl, S. R.; Moliterno, D. J. The role of the platelet in the pathogenesis of atherothrombosis. *Am. J. Cardiovasc. Drugs* **2005**, *5*, 399–408.
- (8) (a) Kumar, A.; Villani, M. P.; Patel, U. K.; Keith, J. C.; Schaub, R. G. Recombinant soluble form of PSGL-1 accelerates thrombolysis and prevents reocclusion in a porcine model. *Circulation* **1999**, *99*, 1363–1369. (b) Bienvenu, J. G.; Tanguay, J. F.; Theoret, J. F.; Kumar, A.; Schaub, R. G.; Merhi, Y. Recombinant soluble P-selectin glycoprotein ligand-1-Ig reduces restenosis through inhibition of platelet-neutrophil adhesion after double angioplasty in swine. *Circulation* **2001**, *103*, 1128–1134.
- (9) Beeh, K. M.; Beier, J.; Meyer, M.; Buhl, R.; Zahlten, R.; Wolff, G. *Pulm. Pharmacol. Ther.* **2006**, *19*, 233–241.
- (10) (a) Mertens, P.; Maes, A.; Nuyts, J.; Belmans, A.; Desmet, W.; Esplugas, E.; Charlier, F.; Figueras, J.; Sambucetti, G.; Schwaiger, M.; Mortelmans, L.; Van de Werf, F. *Am. Heart J.* **2006**, *152*, e125/1–e125/8. (b) www.clinicaltrials.gov
- (11) Kerr, K. M.; Auger, W. R.; Marsh, J. J.; Comito, R. M.; Fedullo, R. L.; Smits, G. J.; Kapelanski, D. P.; Fedullo, P. F.; Channick, R. N.; Jamieson, S. W.; Moser, K. M. *Am. J. Respir. Crit. Care Med.* **2000**, *162*, 14–20.
- (12) Wakita, H.; Ruetzler, C.; Illoh, K. O.; Chen, Y.; Takanohashi, A.; Spatz, M.; Hallenbeck, J. M. *J. Cereb. Blood Flow Metab.* **2008**, *8*, 341–353. (b) *E-Selectin Nasal Spray to Prevent Stroke Recurrence*. NCT00012454, www.clinicaltrials.gov/ct2/show/NCT00012454.
- (13) Seekamp, A.; van Griensven, M.; Dhondt, E.; Diefenbeck, M.; Demeyer, I.; Vundelinckx, G.; Haas, N.; Schaechinger, U.; Wolowicka, L.; Rammelt, S.; Stroobants, J.; Marzi, I.; Brambrink, A. M.; Dziurdzik, P.; Gasiorowski, J.; Redl, H.; Beckert, M.; Khan-Boluki, J. *Crit. Care Med.* **2004**, *32*, 2021–2028.
- (14) Rossi, B.; Constantin, G. *Inflammation Allergy: Drug Targets* **2008**, *7*, 85–93.
- (15) Kaila, N.; Janz, K.; DeBernardo, S.; Bedard, P. W.; Camphausen, R. T.; Tam, S.; Tsao, D. H. H.; Keith, J. C., Jr.; Nickerson-Nutter, C.; Shilling, A.; Young-Sciame, R.; Wang, Q. Synthesis and biological evaluation of quinoline salicylic acids as P-selectin antagonists. *J. Med. Chem.* **2007**, *1*, 21–39.
- (16) (a) Kaila, N.; Janz, K.; Huang, A.; Moretto, A.; DeBernardo, S.; Bedard, P. W.; Tam, S.; Clerin, V.; Keith, J. C., Jr.; Tsao, D. H. H.; Sushkova, N.; Shaw, G. D.; Camphausen, R. T.; Schaub, R. G.; Camphausen, R. T.; Wang, Q. 2-(4-Chlorobenzyl)-3-hydroxy-7,8,9,10-tetrahydrobenzo[H]quinoline-4-carboxylic Acid (PSI-697): Identification of a Clinical Candidate from the Quinoline Salicylic Acid Series of P-Selectin Antagonists. *J. Med. Chem.* **2007**, *1*, 40–64. (b) Chelliah, R.; Lucking, A. J.; Tattersall, L.; Daga, S.; Beresford-Cleary, N. J.; Cortas, K.; Fox, K. A. A.; Feuerstein, G. Z.; Connolly, T. M.; Newby, D. E. P-Selectin antagonism reduces thrombus formation in humans. *J. Thromb. Haemostasis* **2009**, *7*, 1915–1919.
- (17) (a) Cragoe, E. J.; Robb, C. M.; Bealor, M. D. The synthesis of 3-hydroxycinchoninic acid and certain of its derivatives. *J. Org. Chem.* **1953**, *18*, 552–560. (b) Cragoe, E. J.; Bealor, M. D.; Robb, C. M.; Ziegler, C.; Sprague, J. M. The synthesis of 3-hydroxy-2-phenylquinoline-4,8-dicarboxylic acid and certain of its derivatives. *J. Org. Chem.* **1953**, *18*, 561–569.
- (18) (a) Sandmeyer, T. Isonitrosoacetanilides and their condensation to form isatin derivatives. *Helv. Chim. Acta* **1919**, *2*, 234–242. (b) Yang, K.; Campbell, B.; Birch, G.; Williams, V. E.; Lemieux, R. P. Induction of a ferroelectric SC* liquid crystal phase by an atropisomeric dopant derived from 4,4'-dihydroxy-2,2'-dimethyl-6,6'-dinitrophenyl. *J. Am. Chem. Soc.* **1996**, *118*, 9557–9561. (c) Marvel, C. S.; Hiers, G. S. Isatin. *Org. Synth.* **1925**, *V*, 71–74.
- (19) Lisowski, V.; Robba, M.; Rault, S. Efficient synthesis of novel 3-(Het)arylthranilic acids via a Suzuki cross-coupling reaction of 7-iodoisatin with (Het)arylboronic acids in water. *J. Org. Chem.* **2000**, *65*, 4193–4194.
- (20) Ezquerro, J.; Pedregal, C.; Lamas, C.; Barluenga, J.; Perez, M.; Garcia-Martin, M. A.; Gonzalez, J. M. Efficient Reagents for the Synthesis of 5-, 7-, and 5,7-Substituted Indoles Starting from Aromatic Amines: Scope and Limitations. *J. Org. Chem.* **1996**, *61*, 5804–5812.

- (21) Hewawasam, P.; Meanwell, N. A. A general method for the synthesis of isatins: preparation of regiospecifically functionalized isatins from anilines. *Tetrahedron Lett.* **1994**, *35*, 7303–7306.
- (22) Wissner, A. 2-Heterosubstituted silylated ketone acetals: reagents for the preparation of alpha-functionalized methylketones from carboxylic acid chlorides. *J. Org. Chem.* **1979**, *44*, 4617–4622.
- (23) Fedorynski, M.; Jonczyk, A. Synthesis of 1-arylcyclopropanecarbonitriles under phase-transfer catalytic conditions. *Org. Prep. Proc. Int.* **1995**, *27*, 355–359.
- (24) (a) Kaila, N.; Somers, W. S.; Thomas, B. E.; Janz, K.; Thakker, P.; DeBernardo, S.; Tam, S. Y.; Yang, R.; Moore, W.; Wrona, W.; Bedard, P. W.; Crommie, D.; Tsao, D.; Alvarez, J. C.; Keith, J.; Alvarez, J. C.; Ni, H.; Wagner, D. D.; Marchese, E.; Patton, J. T.; Magnani, J. L.; Camphausen, R. T. Quinic acid derivatives as sialyl Lewisx-mimicking selectin inhibitors: design, synthesis and crystal structure in complex with E-selectin. *J. Med. Chem.* **2005**, *48*, 4346–4357 and references therein. (b) Kumar, A.; Villani, M. P.; Patel, U. K.; Keith, J. C., Jr.; Schaub, R. G. Recombinant soluble form of PSGL-1 accelerates thrombolysis and prevents reocclusion in a porcine model. *Circulation* **1999**, *99*, 1363–1369. (c) Khor, P. S.; McCarthy, K.; Dupont, M.; Murray, K.; Timony, G. Pharmacokinetics, pharmacodynamics, allometry, and dose selection of rPSGL-Ig for phase I trial. *J. Pharmacol. Exp. Ther.* **2000**, *293*, 618–624. (d) Kogan, T. P.; Dupre, B.; Bui, H.; McAbee, K. L.; Kassir, J. M.; Scott, I. L.; Hu, X.; Vanderslice, P.; Beck, P. J.; Dixon, R. A. F. Novel synthetic inhibitors of selectin-mediated cell adhesion: synthesis of 1,6-bis[3-(3-carboxymethylphenyl)-4-(2-R-D-mannopyranosyloxy)phenyl]hexane (TBC1269). *J. Med. Chem.* **1998**, *41*, 1099–1111. (e) Langer, R.; Wang, M.; Stepkowski, S. M.; Hancock, W. W.; Han, R.; Li, P.; Feng, L.; Kirken, R. A.; Berens, K. L.; Dupre, B.; Podder, H.; Dixon, R. A. F.; Kahan, B. D. Selectin inhibitor bimosiamose prolongs survival of kidney allografts by reduction in intra-graft production of cytokines and chemokines. *J. Am. Soc. Nephrol.* **2004**, *15*, 2893–2901. (f) Abraham, W. M.; Ashfaq Ahmed, A.; Sabater, J. R.; Lauredo, I. T.; Botvinnikova, Y.; Bjerkke, R. J.; Hu, X.; Revelle, M. B.; Kogan, T. P.; Scott, I. L.; Dixon, R. A. F.; Yeh, E. T. H.; Beck, P. J. Selectin blockade prevents antigen-induced late bronchial responses and airway hyperresponsiveness in allergic sheep. *Am. J. Respir. Crit. Care Med.* **1999**, *159*, 1205–1214. (g) Since the in vitro concentration at which selectin inhibitors are active is very high, solubility is limiting for many compounds at the higher concentrations necessary to generate a full concentration curve and IC₅₀. So determination of an IC₅₀ was only done for compounds with greater or equal to 50% inhibition at 250 μM.
- (25) Ley, K.; Bullard, D. C.; Arbones, M. L.; Bosse, R.; Vestweber, D.; Tedder, T. F.; Beaudet, A. L. Sequential contribution of L- and P-selectin to leukocyte rolling in vivo. *J. Exp. Med.* **1995**, *181*, 669–675.
- (26) Mayer, M.; Meyer, B. Characterization of ligand binding by saturation transfer difference NMR spectroscopy. *Angew. Chem., Int. Ed.* **1999**, *38*, 1784.
- (27) Hicks, A. E. R.; Leppanen, A.; Cummings, R. D.; Mcever, R. P.; Hellewell, P. G.; Norman, K. E. Glycosulfopeptides modeled on P-selectin glycoprotein ligand 1 inhibit P-selectin-dependent leukocyte rolling in vivo. *FASEB J.* **2000**, *16*, 1461–1462.
- (28) (a) Bedard, P. W.; Clerin, V.; Sushkova, N.; Tchernychev, B.; Antrilli, T.; Resmini, C.; Keith, J. C., Jr.; Hennen, J. K.; Kaila, N.; DeBernardo, S.; Janz, K.; Wang, Q.; Crandall, D. L.; Schaub, R. G.; Shaw, G. D.; Carter, L. L. Characterization of the novel P-selectin inhibitor PSI-697 [2-(4-chlorobenzyl)-3-hydroxy-7,8,9,10-tetrahydrobenzo[h]quinoline-4-carboxylic acid] in vitro and in rodent models of vascular inflammation and thrombosis. *J. Pharmacol. Exp. Ther.* **2008**, *324*, 497–506. (b) Chelliah, R.; Lucking, A. J.; Tattersall, L.; Daga, S.; Beresford-Cleary, N. J.; Cortas, K.; Fox, K. A. A.; Feuerstein, G. Z.; Connolly, T. N.; Newby, D. E. P-Selectin antagonism reduces thrombus formation in humans. *J. Thromb. Haemostasis* **2009**, *7*, 1915–1919.
- (29) Robinson, S. D.; Frenette, P. S.; Rayburn, H.; Cumiskey, M.; Ullman-Cullere, M.; Wagner, D. D.; Hynes, R. O. Multiple, targeted deficiencies in selectins reveal a predominant role for P-selectin in leukocyte recruitment. *Proc. Natl. Acad. Sci. U.S.A.* **1999**, *96*, 11452–11457.
- (30) Schmidtke, D. W.; Diamond, S. L. Direct observation of membrane tethers formed during neutrophil attachment to platelets or P-selectin under physiological flow. *J. Cell. Biol.* **2000**, *149*, 719–730.
- (31) Clowes, A. W.; Reidy, M. A.; Clowes, M. M. Mechanisms of stenosis after arterial injury. *Lab. Invest.* **1983**, *49*, 208–215.
- (32) Hayashi, S.; Watanabe, N.; Nakazawa, K.; Suzuki, J.; Tsushima, K.; Tamatani, T.; Sakamoto, S.; Isobe, M. Roles of P-selectin in inflammation, neointimal formation, and vascular remodeling in balloon-injured rat carotid arteries. *Circulation* **2000**, *102*, 1710–1717.
- (33) Meier, T. R.; Myers, D. D., Jr.; Wroblewski, S. K.; Zajkowski, P. J.; Hawley, A. E.; Bedard, P. W.; Ballard, N. E.; Londy, F. J.; Kaila, N.; Vlasuk, G. P.; Schaub, R. G.; Wakefield, T. W. Prophylactic P-selectin inhibition with PSI-421 promotes resolution of venous thrombosis without anticoagulation. *Thromb. Haemostasis* **2008**, *99*, 343–351.
- (34) (a) Myers, D. D., Jr.; Wroblewski, S. K.; Longo, C.; Bedard, P. W.; Kaila, N.; Shaw, G. D.; Londy, F. J.; Rohrer, S. E.; Fex, B. A.; Zajkowski, P. J.; Meier, T. R.; Hawley, A. E.; Farris, D. M.; Ballard, N. E.; Henke, P. K.; Schaub, R. G.; Wakefield, T. W. Resolution of venous thrombosis using a novel oral small-molecule inhibitor of P-selectin (PSI-697) without anticoagulation. *Thromb. Haemostasis* **2007**, *9*, 400–407. (b) Ramacciotti, E.; Myers, D. D.; Wroblewski, S. K.; Deatrick, K. B.; Londy, F. J.; Rectenwald, J. E.; Henke, P. K.; Schaub, R. G.; Wakefield, T. W. P-selectin/PSGL-1 Inhibitors versus enoxaparin in the resolution of venous thrombosis: a meta-analysis. *Thromb. Res.* **2009**, *125*, e138–e142.
- (35) Green, N.; Hu, Y.; Janz, K.; Li, H.-Q.; Kaila, N.; Guler, S.; Thomason, J.; Joseph-McCarthy, D.; Tam, S. Y.; Hotchandani, R.; Wu, J.; Huang, A.; Wang, Q.; Leung, L.; Pelker, J.; Marusic, S.; Hsu, S.; Telliez, J.-B.; Hall, P.; Cuzzo, J. W.; Lin, L.-L. Inhibitors of Tumor Progression Loci-2 (Tpl2) Kinase and Tumor Necrosis Factor α (TNF-α) Production: Selectivity and in Vivo Antiinflammatory Activity of Novel 8-Substituted-4-anilino-6-aminoquinoline-3-carbonitriles. *J. Med. Chem.* **2007**, *50*, 4728–4745.
- (36) Di, L.; Kerns, E.; Li, S.; Carter, G. Comparison of Cytochrome P450 Inhibition Assays for Drug Discovery Using Human Liver Microsomes With LC-MS, rhCYP450 Isozymes with Fluorescence, and Double Cocktail With LC-MS. *Int. J. Pharm.* **2007**, *335*, 1–11.
- (37) Kerns, E. H.; Li, D.; Petusky, S.; Farris, M.; Ley, R.; Jupp, P. Combined Application of Parallel Artificial Membrane Permeability Assay and Caco-2 Permeability Assays in Drug Discovery. *J. Pharm. Sci.* **2004**, *93*, 1440–1453.